Journal of Archaeological Science: Reports

Archaeometric analysis of building ceramics and ‘dolia defossa’ from the Roman Imperial estate of Vagnari (Gravina in Puglia, Italy)

--Manuscript Draft--

Manuscript Number:	
Article Type:	Research Paper
Keywords:	Roman; excavation; economy; Archaeometry; ceramic analysis; provenance determination
Corresponding Author:	Luciana Randazzo University of Calabria Arcavacata di Rende (CS), ITALY
First Author:	Giuseppe Montana, Ph.D.
Order of Authors:	Giuseppe Montana, Ph.D.
	Luciana Randazzo, Ph.D.
	Donatella Barca, Ph.D.
	Maureen Carroll, Ph.D.
Abstract:	This paper concerns the archaeometric analysis of ceramic finds dating to the Roman Imperial period, brought to light during the excavation campaigns conducted at Vagnari (Puglia) in south-east Italy. On the site of the central village (vicus) of this imperial estate, established by the Roman Emperor in the early 1 st century A.D., large dolia (wine vats) sunk into the floor of a winery of the 2 nd century A.D. recently were brought to light. Other discoveries include kilns for the production of ceramic roof tiles and also kiln waste such as misfired tiles. The purpose of the analytical approach was therefore twofold: 1) to establish the composition of local ceramic products and of raw clay resources available nearby; 2) to prove that the dolia were imported and not produced locally (as macroscopic observations of the ceramic vessels would suggest) and to offer a hypothesis concerning their provenance through petrographic observations and chemical analysis. The results show that roof tiles for the settlement were manufactured locally from readily available clay deposits, but the dolia were imported, by sea and/or land, from distant workshops in volcanic zones on the west coast of Italy around Rome or south of Rome near Minturno on the Campanian border.

Highlights

- Petrochemical analysis of tiles and *dolia defossa* (Roman Imperial period)
- Building ceramics for local use manufactured by sourcing nearby clay deposits
- New hypothesis concerning *dolia* production sites in Italy
- New insight into Roman wine storage and supply dynamics

Archaeometric analysis of building ceramics and '*dolia defossa*' from the Roman Imperial estate of Vagnari (Gravina in Puglia, Italy)

G. Montana[1a], L. Randazzo[2a*], D. Barca[2], M. Carroll[3]

[1] Dipartimento di Scienze della Terra e del Mare (DiSTeM), Università degli Studi Palermo (Italy)
[2] Dipartimento di Biologia, Ecologia e Scienze della Terra (DiBEST), Università della Calabria (Italy)
[3] Department of Archaeology, University of York, (United Kingdom)

[a]These Authors contributed equally to this study.
[*]corresponding author:
L. Randazzo - Dipartimento di Biologia, Ecologia e Scienze della Terra (DiBEST), Università della Calabria, Ponte P. Bucci, Cubo 12B, Arcavacata di Rende, CS (Italy)
luciana.randazzo@unical.it

Abstract

This paper concerns the archaeometric analysis of ceramic finds dating to the Roman Imperial period, brought to light during the excavation campaigns conducted at Vagnari (Puglia) in south-east Italy. On the site of the central village (*vicus*) of this imperial estate, established by the Roman Emperor in the early 1st century A.D., large *dolia* (wine vats) sunk into the floor of a winery of the 2nd century A.D. recently were brought to light. Other discoveries include kilns for the production of ceramic roof tiles and also kiln waste such as misfired tiles. The purpose of the analytical approach was therefore twofold: 1) to establish the composition of local ceramic products and of raw clay resources available nearby; 2) to prove that the *dolia* were imported and not produced locally (as macroscopic observations of the ceramic vessels would suggest) and to offer a hypothesis concerning their provenance through petrographic observations and chemical analysis. The results show that roof tiles for the settlement were manufactured locally from readily available clay deposits, but the *dolia* were imported, by sea and/or land, from distant workshops in volcanic zones on the west coast of Italy around Rome or south of Rome near Minturno on the Campanian border.

Key words: Roman, excavation, economy, archaeometry, ceramic analysis, provenance determination

1. Archaeological Background and Aims

From the 4th century B.C., the growing city-state of Rome embarked on a series of aggressive campaigns of annexation of independent territories in Italy. One of these regions was Apulia (modern Puglia) in the south-east of the peninsula, traditionally a zone of commercial and cultural exchange, due to its geographic position and access to Italic peoples in the west and north, to the Greek colonies on the Ionian coast in the south, and to the Illyrians and mainland Greeks across the Adriatic Sea to the east. Central and eastern Apulia was inhabited by the Italic Peuceti whose major settlement at Botromagno (today Gravina in Puglia) was sacked by the Romans in 306 B.C. (Diodorus Siculus 20.80). From the 3rd century, life temporarily ceased at Botromagno, and it also ended at other smaller Peucetian settlements (Small 1992; Small 2001; Lambrugo and Pace 2017; Depalo 2017). Excavations by the University of Sheffield have shown that a rural settlement at Vagnari also was abandoned at this time (Carroll 2019), but the second century B.C. ushered in a new phase of occupation here as a result of the Roman exploitation of the land (Fig. 1).

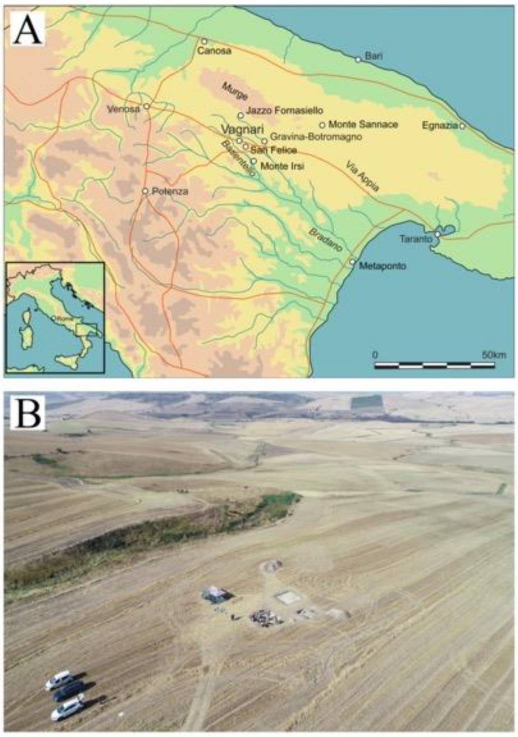

Figure 1. A) Map showing the location of Vagnari in southern Italy (Drawn by I. De Luis); B) Drone image of the *vicus* excavation on the Vagnari plateau and the ravine from which the raw clay samples were taken (Photo by G. Ceraudo and V. Ferrari).

In the early 1st century A.D., the Roman Emperor acquired the land at Vagnari and expanded it to encompass an area of at least 25 sq km, as indicated by field-walking and surface collection of material (Small 2011; C. Small 2011). Roof tile fragments found at Vagnari and the vicinity were stamped with the name of an imperial slave (*Gratus Caesaris*) responsible for tile production, confirming that the estate was indeed owned by Rome's highest ranked citizen (Small et al. 2003). Its purpose was to generate revenues for the imperial coffers. At the heart of the estate at Vagnari lay the central village (*vicus*) through which it was managed. This imperial settlement had a diverse economy, ranging from cereal crop cultivation and sheep grazing and transhumance management, to ceramic building tile and pottery(?) production, and metal-working, especially in the 2nd and 3rd centuries A.D. (Figs. 2A-B). An important addition to the *vicus* in the 2nd century was a *cella vinaria*, or winery, indicating indirectly that vineyards were part of the imperial exploitation of the landscape and that the production of wine had become a staple of the estate economy (Carroll 2016).

The wine at Vagnari was stored in up to 18 globular wine vats (*dolia defossa*), each with a capacity of several hundred litres, inserted in rows into the mortar floor of the winery, of which only ten have left traces archaeologically in the ground (Fig. 2C). These are large vats, but not as large as the enormous transport *dolia* carrying up to 3000 litres each on specially built tanker ships plying the western Mediterranean (Dell'Amico and Pallarés 2005; Sciallano and Marlier 2008; Heslin 2011). The *dolia* at Vagnari were permanently buried up to their necks in the ground, in accordance with Roman agrarian customs, thereby keeping the temperature of the wine constant and cool, a necessary measure in hot climate zones (Pliny the Elder, *Natural History* 14.27). The unroofed storage room of the winery was modest in size, measuring 5.50 by 8.20 m internally (ca. 45 sq m.). It compares roughly in size to some private wineries in the Vesuvius region, such as the Villa Carmiano at Stabiae (6 x 8 m, with at least 12 *dolia*) and the Villa Regina at Boscoreale (6.60 x 8.47 m, with 18 *dolia*), but was much smaller than a contemporary *cella vinaria* at the rural villa of San Giusto in Puglia (6.10 x 14.40 m, with 26 *dolia*) (De Caro 1994; Pietropaolo 1998; Bonifacio 2004).

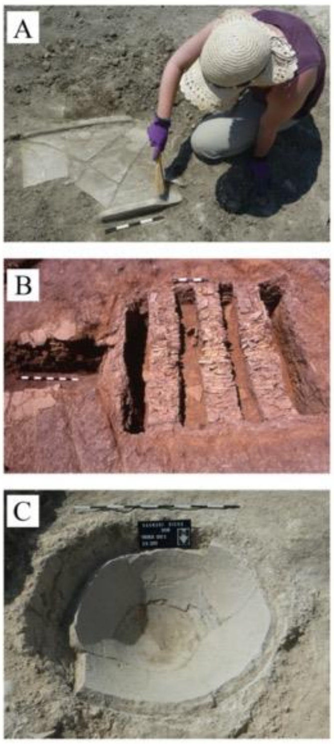

Figure 2. A) Excavating a Roman roof tile (*tegula*) at Vagnari (Photo M. Carroll); B) An excavated Roman tile kiln (Kiln 2) at Vagnari (Photo A.M. Small); C) Remains of a Roman *dolium* inserted in the floor of the winery at Vagnari (Photo M. Carroll).

By the middle of the 3rd century, the Vagnari winery appears to have gone out of use, and the *dolia* were either removed completely, to be re-used elsewhere, as in the Villa of Augustus at Somma Vesuviana, or smashed into pieces to be used secondarily as building material, as they were at the villa of Settefinestre (Celuzza 1985; Aoyagi et al. 2018).

This paper concerns the archaeometric analysis of a wide set of ceramic finds representative of both *dolia* and locally produced roof tiles. The collected ceramic sherds were all subjected to petrographic analysis (thin-section microscopy) and chemical analysis (ICP-EOS + ICP-MS), together with clay samples representative of the raw materials available near the settlement (subjected to experimental firing). Some *dolia* samples (VD-4, VD-5, VD-6, VD-7 and VD-8) were selected for the chemical analysis of the clinopyroxenes contained in the paste, by SEM-EDS (major elements) and ICP-MS Laser Ablation (trace elements). The objectives of the analyses are both the compositional characterization of local ceramic pastes and the identification of the production area of the *dolia*, which appear as imported products even at the scale of macroscopic observation due to the presence of coarse volcanic inclusions.

2. Geological setting

The Murge Plateau is a large tabular relief, elongated in the same direction as the Bradanic Foredeep (which delimits it to the south-east) and gradually degrading to the north-east towards the Adriatic Sea. From a lithological point of view, the north-western Murge is distinguished by the presence of extensive outcrops of carbonate rocks from the Cretaceous period (such as the platform limestones belonging to the "Calcare di Bari" and "Calcare di Altamura" formations). The shallow-water Plio-Pleistocene calcarenites known as "Calcareniti di Gravina" lay with angular discordance on the Cretaceous limestones.

The settlement of Vagnari is located in the Basentello valley about 15 km west of the town of Gravina (ancient Botromagno), in a strategic location near the Roman road, the Via Appia. The study area is a large plateau of deposits uplifted during the mid- to late Pleistocene and it

consists of a spectrum of depositional environments from deep water marine through shallow coastal to shoreline (beach) conditions of coastal and marine origin. Geologically, these deposits are part of the Adriatic – Bradanic Foredeep (Pieri et al. 2012). Marine deposits, primarily marls of upper Pliocene age, are overlain by marly clay hemi-pelagites (Argille Subappennine Formation) and coarse-grained regressive coastal deposits.
In particular, the area between the town of Gravina and the Masseria Vagnari, the modern agricultural estate on which the Roman site is located, according to the geological surveys of the surface (Azzaroli et al., 1968), is characterized by Plio-Pleistocene deposits consisting of: 1) silty clays with an important microfaunistic content, represented by benthic and planktonic foraminifera (“Argille Subappennine”, locally also known as “Argille di Gravina”); 2) calcareous-quartz sands with arenaceous and fossiliferous levels; 3) polygenic conglomerates with pebbles of crystalline rocks; 4) fine quartz-micaceous sands. Near the town of Gravina, the Pleistocene (Calabrian) fossiliferous calcarenite known as "Tufo di Gravina" crops out. The area is also characterized by the presence of extensive Pleistocene and Holocene alluvial terraced deposits mainly composed of clayey silts with sand and pebble levels (Fig. 3A).

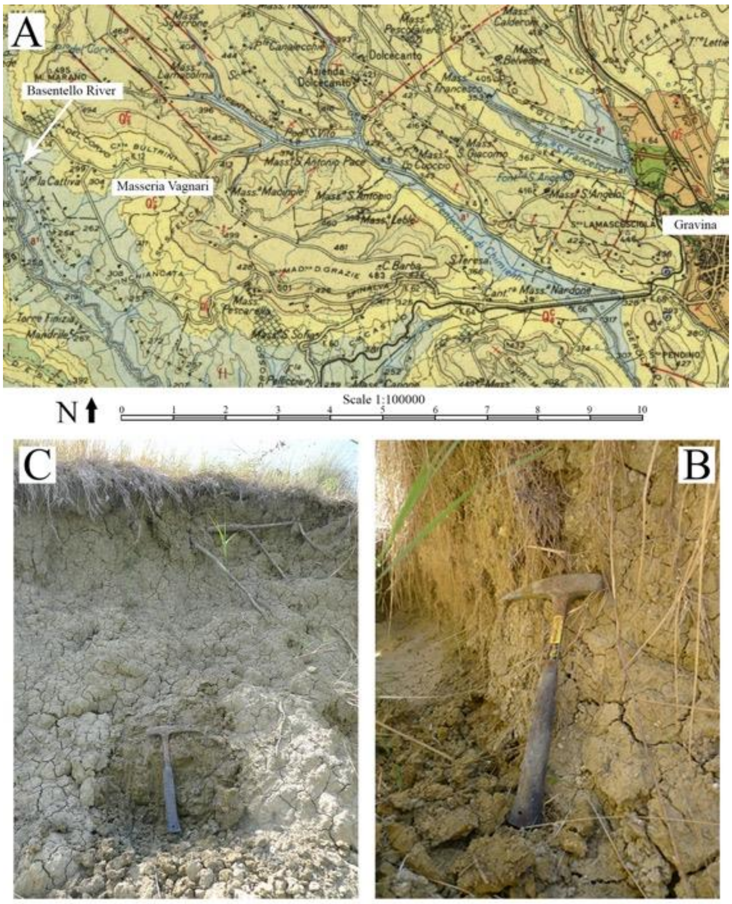

Figure 3. A) Geological map of the area of Vagnari (simplified after Foglio 188 – Gravina di Puglia, Azzaroli et al., 1968). Codes of Formations that outcrop in the territory of Vagnari are provided here: Q_a^C = Argille Subappennine, locally also known as Argille di Gravina; Q_s^C = Sabbie di Monte Marano (calcareous-quartz sands with arenaceous and fossiliferous levels); Q_c^C = Pleistocene (Calabrian) fossiliferous calcarenite known as "Tufo di Gravina"; f^l = Pleistocene alluvial terraced deposits; a^1 = Holocene alluvial terraced deposits. The full legend is accurately reported in Azzaroli et al., 1968; B) VC-1 sampling point; B) VC-2 sampling point.

Therefore, in light of the geological evidence, it is possible to state that in the immediate vicinity of the Masseria Vagnari geological deposits are easily available from which the raw material for ceramic production can be supplied (Apennine clays and alluvial deposits).

3. Material sampling and analytical methods

In order to define the compositional features of locally produced tiles and the imported *dolia* recovered at the site, representative samples of both the ceramic classes were selected. Twenty-four ceramic samples were selected from a large number of ceramic sherds that had been carefully examined by visual analysis to be subjected to the analytical routine. Twelve tile samples, 10 *dolia* samples and 2 pieces of overfired kiln waste (tiles) were considered (Tab. 1). Moreover, clayey raw materials were sampled after a geological field survey in the close vicinity of the site. These clay deposits occur at several points near the settlement, especially along the alluvial dumps of the Basentello River. Clayey materials were carefully collected from a fresh surface, and any soil covers were removed beforehand (Figs. 3B-C).
The raw clays (after air-drying and quartering routines) were mixed with water and molded into experimental briquettes, then oven-dried fired in a muffle furnace at increasing temperature, 700°C, 800°C, 900°C, under fully oxidant conditions (Tab. 1, Fig. 4).

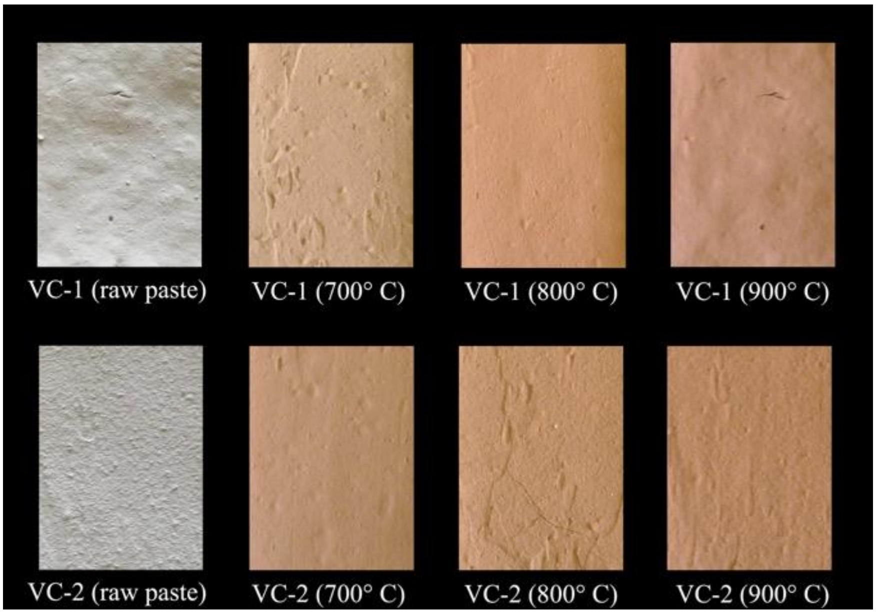

Figure 4. Clayey materials experimental briquettes after firing test.

Thin-sections were made from the fired experimental briquettes to be observed under a polarizing microscope and compared with the archaeological ceramic sherds in order to identify local production by the petrographic markers. The petrographic markers are represented by the main compositional and textural characteristics involving both aplastic inclusions and groundmass which are currently used for the definition of a given ceramic paste group. (Montana 2020). For thin-section microscopy, a Leica DC 200 polarizing microscope equipped with a digital camera was employed. The relative abundance of non-plastic inclusions (modal composition) was carried out at a semi-quantitative level and expressed through ordinal variables (frequency intervals), through conventional point counting techniques (Matthews et al. 1991).
Bulk chemical compositions of ceramic samples were determined by the Activation Laboratories Ltd. (Ontario, Canada), using the fusion inductively coupled plasma optical emission spectrometry (ICP-OES) technique for major oxides and inductively coupled plasma mass spectrometry (ICP-MS) for trace elements (Package 4LITHO). The samples were run for major oxides and selected trace elements on a combination simultaneous/sequential Thermo Jarrell-Ash ENVIRO II ICP or a Varian Vista 735 ICP. Fifty-six elements were here considered

with detection limits in brackets): Na (0.01), Mg (0.01), Al (0.01), Si (0.01), P (0.01), K (0.01), Ca (0.01), Ti (0.001), Mn (0.001) and Fe (0.01), given as oxides (mass%), and Cr (20), V (5), Cu (10), Zn (30), Rb (2), Sr (2), Y (1), Zr (2), Ba (2), Pb (5), Ce (0.1), Nb (1), La (0.1), Sc (1), Be (1), V (5), Y (2), Co (1), Ga (1), Ge (1), As (5), Mo (2), Ag (0.5), In (0.2), Sn (1), Sb (0.5), Cs (0.5), Pr (0.05), Nd (0.1), Sm (0.1), Eu (0.05), Gd (0.1), Tb (0.1), Dy (0.1), Ho (0.1), Er (0.1), Tm (0.05), Yb (0.1), Lu (0.01), Hf (0.2), Ta (0.1), W (1), Tl (0.1), Bi (0.4), Th (0.1), U (0.1) and Ni (20), given as element (ppm). The results concerning the major elements oxides were recalculated on LOI-free basis.

Micro-chemical analyses were carried out on selected *dolia* samples (VD-4, VD-5, VD-6 and VD-7), in order to define the composition of the clinopyroxene crystal present in the ceramic paste. Major elements were determined by an Electron Probe Micro Analysis (EPMA) JEOL-JXA 8230 coupled with 5 WDS Spectrometers XCE type equipped with a LDE, TAP, LIF and PETJ analyzing crystal. Working conditions were: 15 KeV HV; 10 nA probe current; 11 mm working distance; ZAF quant correction. A variety of mineral standards (jadeite, olivine, diopside, orthoclase, tugtupite, pyrite and galena) and pure metals (Fe, Ti, Mn) were used for calibration and quality control. For measuring trace elements concentration (Sc, V, Sr, Y, Zr, La, Ce, Pr, Nd, Sm, Eu, Gd, Tb, Dy, Er, Tm, Yb and Lu) the Laser ablation ICP-MS technique was employed, by using a Elan DRC-e (Perkin Elmer SCIEX—Canada) plasma mass spectrometer, coupled with a New Wave UP213 (solid state Nd–YAG laser operating at a wavelength of 213 nm). Analyses were performed on 80 μm thin cross sections. Calibration was obtained on standard glass NIST SRM612 (trace elements at nominal concentrations of 50 ppm after Pearce et al. 1997). CaO concentrations, obtained from previous quantitative electron microprobe analyses, were used as internal standardization to correct instrumental instability. Ablation was performed by 50 μm spots, with a constant laser repetition rate of 10 Hz and fluence of ~20 J/cm^2. In all analyses, a transient signal of intensity vs. time was obtained for each element using a 60 s background level (acquisition of gas blanks) followed by 40 s of ablation and then 60 s of post-ablation at background levels. Data were processed by the Glitter program. Accuracy was evaluated on BCR 2G Basalt Glass reference material, and the resulting element concentrations were compared with reference values from the literature (Gao et al. 2002). Accuracy, as the relative difference from reference values, was always better than 10%. A minimum of three spot analyses for each clinopyroxene crystal were performed and the average was considered for the final elemental concentration.

4. Results and discussion

4.1 Petrography

The results derived from the observation by polarized light microscopy of all the ceramic samples (24) and the experimental firing tests obtained from on-site available plastic clayey raw materials (6 samples in total) are reported in detail in Supplementary Material – Table S1. Specifically, results relating to local production (primarily represented by roof tiles, kiln waste, and firing tests) are commented on below. Following this, the petrographic results relating to the *dolia* are discussed.

4.1.1 Ceramic tiles, tile waste and experimental clay briquettes

The cross-examination of the data reported in Supplementary Material – Table S1, specifically concerning kiln waste (samples: VW-1, VW-2), tiles (samples: VT-1, VT-2, VT-3, VT-4, VT-5, VT-6, VT- 7, VT-8, VT-9, VT-10, VT-11, VT-12), and firing tests obtained from the on-site available raw clay (samples: VC-1A, VC-1B, VC-1C, VC-2A, VC-2B, VC-2C), allows us to report a more than satisfactory match in terms of their textural and compositional

characteristics. Consequently, this can be assumed as representative of local ceramic production (at least during the 2nd and 3rd centuries A.D.).
From the textural point of view, this locally produced ceramic paste is characterized by a moderately homogeneous and serial distribution of aplastic inclusions. The abundance of inclusions (packing) is rather poor (generally not higher than 10% area). They are, moreover, represented by relatively small particles (mainly within 0.06 mm and 0.2 mm in size). In fact, inclusions size ranges from coarse silt (0.04-0.06 mm) to very fine (0.06-0.125 mm) and fine sand (0.125-0.25 mm). Greater sizes are essentially sporadic to rare.
As regards the composition, the aplastic inclusions are mainly composed of monocrystalline quartz (angular grains prevalent), followed by polycrystalline quartz, tiny lamellae of muscovite (both common constituents), and smaller quantities of K-feldspar and plagioclase. Minute clinopyroxene crystals were found as accessory constituents (one or very few individuals) in about the 50% of the samples representative of this ceramic paste. Lithic fragments were also recognized as common constituents or, more frequently, sporadic to rare, being mainly composed of acid crystalline rocks and (subordinately) chert. The calcareous component is well represented (from abundant to common), consisting of microfossils or micrite clots which are the result of (partial/total) transformation of microfossils after the firing process at temperatures higher than 800 °C (Cau Ontiveros et al. 2002; Gliozzo 2020; Maritan 2020). The groundmass (fine plastic matrix) is more often optically inactive and characterized by common lumps. The latter are generally an index of a rough maturation and/or mixing of the raw clay. The pores have mainly an irregular to subregular shape (subrounded cast of microfossils completely decomposed by firing). Most of the observed samples appear to be impregnated by variable quantities of secondary calcite, which precipitated in the pore network during the period in which the sherds were in the ground (Figs. 5A-F).
The comparison between the archaeological finds and the experimental tests deriving from the controlled firing of the clays sampled in the surroundings of the Masseria Vagnari confirmed without any doubt that locally available ceramic raw materials were used. These materials belong to the Apennine Clays Formation, characterized by Upper Pliocene-Calabrian fossil associations, or to terraced fluvio-lacustrine alluvial deposits of the Pleistocene age, consisting of clayey-sandy terraced sediments (Fig. 3A). The characteristics of the Sub-Apennine Clays, well described by Di Pierro (1981) for an area belonging to the Bradanic Foredeep and located about 40 km west of Gravina, are satisfactorily coincident with what has been observed in the materials collected in the vicinity of the Masseria Vagnari. These are gray-blue clays with the fraction less than 63 microns, which represents about 90% of the total (similar quantities of clay and silty fraction). From a mineralogical point of view, the Sub-Apennine Clays consist of clay minerals, carbonates, quartz, feldspar, micas, and iron oxide/hydroxide. Clay minerals are represented by illite, montmorillonite, kaolinite, chlorite, and illite-smectite mixed layers (Di Pierro 1981). It should be flagged up here that the employment of Sub-Apennine Clays and/or Pleistocene alluvial deposits as raw material for ceramic use has been attested recently by Gliozzo and coauthors (2018) at several Apulian archaeological sites located about 60 km north of our site at the Masseria Vagnari.

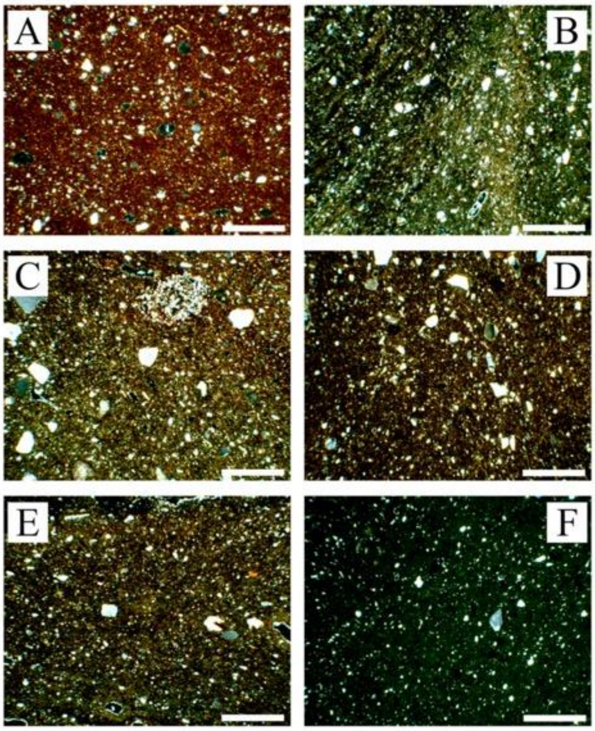

Figure 5. (A) Local raw clay (sample VC1-1) after firing test at 800°C (crossed nicol, scale bar = 0.5 mm); (B) tile sample VT-2 (crossed nicol, scale bar = 0.5 mm); (C) tile sample VT-6 (crossed nicol, scale bar = 0.5 mm); (D) tile sample VT-10 (crossed nicol, scale bar = 0.5 mm); (E) tile sample VT-12 (crossed nicol, scale bar = 0.5 mm); (F) tile waste sample VW-1 (crossed nicol, scale bar = 0.5 mm).

4.1.2 *Dolia*

The samples carefully selected as representative of the *dolia defossa* at Vagnari (VD-1, VD-2, VD-3, VD-4, VD-5, VD-6, VD-7, VD-8, VD-9, VD-10) showed truly comparable compositional and textural characteristics under the polarizing microscope, both in qualitatively (e.g. nature and sorting of aplastic inclusion) and quantitatively (e.g. abundance ratio and grain-size). For this reason, they reasonably may be considered to belong to a single petrographic ceramic paste. Furthermore, no minero-petrographic matching with the above-described local ceramic production and clayey materials (experimental firing tests) could be discerned. Hence, it can be deduced that the *dolia*, which even macroscopically show a distinctive abundance of coarse volcanic inclusions, were unquestionably imported to the site of Vagnari.

On average, this ceramic paste is characterized by a medium-high frequency of aplastic inclusions (prevailing 20-25% area) with an apparent bimodal sorting (Supplementary Material – Table S1). Only samples VD-6 and VD-8 showed serial or serial to bimodal sorting. Coarse and very coarse sand grains (0.5-2 mm) prevail on one mode and very fine grains (0.04-0.1 mm) on the other mode. Maximum grain size (MGS) ranges between 1.3-2.5 mm. This characteristic bimodality supports the suggestion that the raw clay was intentionally tempered by adding coarser sand inclusions, with the purpose of improving the physical and mechanical performances of the finished product. The presence of abundant inclusions of volcanic nature is the peculiar compositional characteristic of this ceramic paste, consisting of both monomineralic grains and lithic fragments. The aplastic inclusions of volcanic origin constitute the most part of the coarser fraction (0.5-2.5 mm) in the ceramic fabric and are unquestionably prevalent over the component of sedimentary origin, which is limited to the finest sand fraction (mainly 0.06-0.2 mm). As far as the monomineralic volcanic grains are concerned, clinopyroxene prevails over sanidine (generally common to sporadic component) in almost all cases. Only the samples coded VD-6 and VD-8 (subordinately, with respect to VD-6) showed slight divergence, the sanidine being relatively more abundant than clinopyroxene and also represented by large subhedral crystals (rarely twinned). Plagioclase, amphibole, biotite, garnet, opaque minerals, leucite, olivine, apatite, and titanite are sporadic to rare constituents, by far less abundant with respect to the above-mentioned phases. Among the volcanic lithic fragments recognized in this ceramic paste, hypo-silicic volcanic rocks such as leucite-bearing tephrites to phonolites are by far the most frequent, while trachytes, trachyphonolites, and latites are subordinate to rare (Figs. 6A-D).

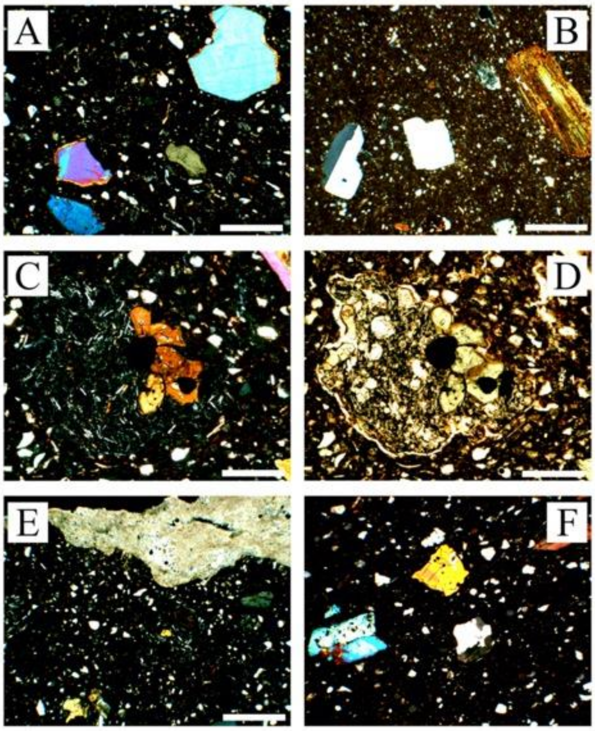

Figure 6. Subhedral clinopyroxenes composing the largest aplastic inclusions in sample VD-2 (crossed nicols, scale bar = 0.5 mm) (A); twinned sanidine and biotite in sample VD-6 (crossed nicols, scale bar = 0.5 mm) (B); augite and opaque oxides cluster in a glomeroporphyritic leucitic tephrite rock fragment, under crossed (C) and parallel nicols (D) (scale bar = 0.2 mm); coating of secondary "burial" calcite in the external surface of sample VD-10 (crossed nicols, scale bar = 0.5 mm) (E); polycrystalline quartz inclusion in sample VD-5 (crossed nicols, scale bar = 0.5 mm) (F).

The finest aplastic inclusions are mostly composed of sedimentary monocrystalline and polycrystalline quartz (common), mica flakes (rare), sericitized K-feldspar (rare), and chert (rare). Furthermore, polymineralic granules composed of quartz, K-felspar, and mica are also part of this sedimentary component (acid crystalline lithic fragments in Supplementary Material – Table S1). Calcareous bioclasts, or rather what remains of them after the firing process (micrite clots and/or cast pores), are poorly represented (Figs. 6E-F). All the above mentioned "detrital" minerals/lithoclasts can be considered as natural (intrinsic) components of the clayey deposit originally used as ceramic raw material. The groundmass is characterized by the presence of clay lumps (deriving from an approximate mix of the raw material) and by the absence of any optical activity. Macropores are mostly represented by shrinkage cracks, which have already formed in the drying phase (before firing), especially at the contact point with the largest aplastic inclusions. It should be emphasized that all the samples are affected by incrustations of secondary calcite with rather variable thickness, up to a maximum of about 1 mm; this is due to the sherds being buried in the ground. Pores in the groundmass are may be partially filled with secondary calcite.
In general, the results derived from thin-section microscopy highlight that this ceramic paste potentially holds significant minero-petrographic markers which might give useful insights for narrowing down the provenance area of the studied *dolia*. In fact, the presence of the aplastic

inclusions of leucite-bearing SiO_2-undersaturated magmatic rock fragments (common to sporadic), together with clinopyroxene (abundant), sanidine (common to sporadic), plagioclase, olivine, amphibole, biotite, and melanite garnet (sporadic to rare), strongly supports the hypothesis of provenance from the wide volcanic region which covers most of the regional territory of Latium, from the Vulsini Mountains and Bolsena Lake areas (Tuscan border) southwards towards to Rome and up to the mouth of the Garigliano River (Campanian border). This territory constitutes the Roman Magmatic Province and the Ernici-Roccamonfina Magmatic Province, and it is markedly characterized by recent (Quaternary) volcanism with prevalent silica undersaturated and ultrapotassic eruptive products belonging to the HKS ultrapotassic volcanic series (after Peccerillo 2005). The mineralogical compositions of these volcanic products match more than satisfactorily with the aplastic inclusions found in the ceramic paste of this study. Relevant to mention here are two recently discovered *dolia defossa* found at San Giovanni (Portoferraio, island of Elba, Italy) during the archaeological excavations of a Roman farm (late 2nd century B.C.-1st century A.D.) that have been attributed to the same volcanic area on the basis of the mineral-petrographic and chemical analyses (Manca et al. 2016). The compositional comparison of the aplastic inclusions between the dolia found on the Island of Elba with those of the Vagnari excavations (minerals and rock fragments) highlights a very good textural matching (grain size distribution and packing) but some compositional differences as well. These latter consist of a different ratio of abundance between K-feldspar and clinopyroxene (relatively more abundant sanidine in the *dolia* of Elba) and, above all, in the classification of the lithic fragments (tephrites and leucite phonolites of the HKS series more abundant in the *dolia* from Vagnari). Other potential provenance areas characterized by volcanic products, and even closer to the site of Vagnari, could be theoretically considered, such as the Campanian and Monte Vulture (Puglia) magmatic provinces. However, the Campanian volcanic products from the Phlegraean Fields, Ischia, and Somma-Vesuvio are characterized by the relative prevalence of silica undersaturated potassic rocks (KS series), ranging from trachybasalt to latite and trachyte, over the products of ultrapotassic series (HKS, leucite tephrite to phonolite). Moreover, in the Roman wine amphorae produced in the 1st century B.C. at Mondragone and in the Falerno region in Campania, a comparatively more abundant detrital sedimentary component was recognized (Thierrin-Michael et al. 2018), compared to the ceramic paste representative of the Vagnari *dolia*. Finally, Monte Vulture, which is located only 80 km north-west of Vagnari, is characterized by volcanic products that are easily distinguishable from the previous ones, above all by the typical presence of hauyna (feldspathoid belonging to the sodalite group), being abundant both as a phenocryst or in the groundmass.

4.2 Chemistry

4.2.1 Ceramic tiles, tile waste and clays

Table 2 shows the concentration values of the major and trace elements relative to the local tiles (VW and VT-series) and to the clayey raw materials (VC-series) sampled near the site of Vagnari. After a rapid comparative examination of all the elemental values (major elements have been normalized against loss on ignition) it is immediately clear that the compositional homogeneity of the pottery produced locally in the imperial age, already highlighted through the microscopic observation of thin-sections, is additionally established by chemical analyses. At the same time, the excellent compositional matching between the building ceramics and the "Apennine Clays" (a good ceramic raw material available at a short distance from the place of use, here represented by samples VC-1 and VC-2) is clearly confirmed. Due to this compositional homogeneity, tiles, kiln waste, and raw clays are hereafter considered as a single

"chemical group". Accordingly, average values can be used as a first significant reference for future discernment of local ceramic productions (even diachronically).
Based on the abundance of the major elements, it is possible to confirm that the local ceramics were produced using "calcareous clays" as raw material. In fact, the average concentration of CaO is equal to 14.50% weight (wt) despite showing a modest variability in the set of samples analysed (variation range = 12.48-17.26% wt, RSD = 10%). The concentration of SiO_2 is represented by an average value of 56.68% with a relatively modest range of variation compared to that of CaO (55.21-57.71% wt, RSD = 2%). The average content of Fe_2O_3 stands at 5.41%, an absolute value that is not particularly high, however, with quite limited variations (5.16-6.23% wt, RSD = 4%). The same considerations can also be extended to Al_2O_3 (mean = 15.37, RSD = 4%), K_2O (mean = 2.81, RSD = 6%) and TiO_2 (mean = 0.71, RSD = 5%) concentrations, both with relatively small variation ranges and more than acceptable RDSs values. All the remaining oxides representative of the major elements, i.e., MgO (mean = 2.63), Na_2O (mean = 1.06) and P_2O_5 (mean = 0.23), are characterized by relatively broad ranges of variation with RSDs ranging from 13% to 15%.
The two representative samples of the local clays (VC-1 and VC-2) show contentment values satisfactorily corresponding to each other, with small differences mostly limited to the CaO content (around 2% on average). The good correspondence of the variation intervals between archaeological ceramic finds and clayey raw material is shown in Fig. 7A.

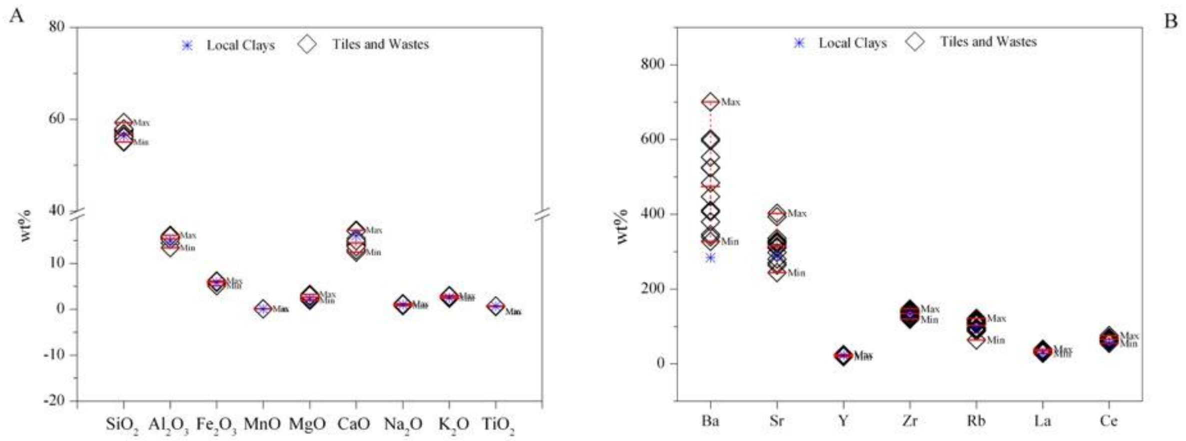

Figure 7. A) Variation intervals of major elements between archaeological ceramic finds and clayey raw material; B) Variation intervals of trace elements between archaeological ceramic finds and clayey raw material.

Between the trace elements no significant chemical markers can be recognized. At the same time, as in the case of the major elements, a good homogeneity of the concentration values within "paste group" is confirmed. In fact, a large number of analysed trace elements show RDSs values below or slightly above 20 %, including V (10%), Ba (20%), Sr (14%), Y (9%), Zr (6%), Rb (16%), La (8%), Ce (8%), Pb (21%), Th (8%), U (13%). Barium (mean = 475 ppm) and Rubidium (mean = 103 ppm) and zirconium are between the relatively more abundant trace elements, whose concentration values could be correlated to the relative incidence of aplastic poly/monomineralic inclusions deriving from acid crystalline rocks (granitoid or metamorphic medium-high grade). The abundance of strontium (mean = 315 ppm), geochemically correlated to the abundance of calcium, is generally linked to the calcareous component of the "ceramic paste". In Fig. 7B the variation intervals of some trace elements selected in the ceramic finds and in the local clayey raw materials (VC-1 and VC-2) are compared. The wide compositional overlap between ceramic products and clay raw materials is apparent for most of the elements here considered, with some slight discrepancies limited to Ba and Sr (potentially coarser temper added to raw clay).

4.2.2 *Dolia* bulk compositions

On the basis of the abundance of the major and trace elements, and in full agreement with what was found during the microscopic observations, the studied *dolia* appear to be an acceptably homogeneous "chemical group" as well (Hein and Kilikoglou 2020). An excellent correlation between the mineral-petrographic and chemical data has accordingly been confirmed.

In general, the RDSs are well below 10% in the case of SiO_2, Al_2O_3, Fe_2O_3 and TiO_2. For MnO, MgO and K_2O they are between 10% and 15%, while CaO, Na_2O and P_2O_5 have RDSs values higher than 15% (Table 3). The SiO_2 content varies from a minimum of 54.75% (VD-6) to a maximum of 61.38% by weight (VD-1), with an average value of 58.88%. An RSD of 4% suggests a good consistency for the analysed set of samples. Equally narrow ranges of variation have been recorded for Al_2O_3, $Fe_2O_{3(T)}$ and TiO_2, with average concentrations of 14.79%, 6.69% and 0.84% (by weight) respectively.

Relatively wider ranges of variation can be observed for alkaline earth metals on the one hand and alkali metals on the other. For MgO an average value of 3.16% by weight has been observed with RDS slightly higher than 10%, while the CaO varies from a minimum of 8.39% by weight (VD-10) up to 14.73% (VD-3) with an average value equal to 11.19% by weight (RDS = 18%). Among the alkali metals K_2O shows a concentration equal to 2.81% by weight (RDS = 15%). It should be emphasized that, unlike all the other samples, only VD-6 shows a visibly different (higher) K_2O value than the average value, i.e. 3.96% by weight (VD-8 only in a minor extent with 2.95 by weight). This result is not surprising at all, considering the differences in terms of abundance of K-feldspar (mainly sanidine) among the aplastic inclusions highlighted only in this sample through microscopic observations (in quantity almost equivalent to clinopyroxene, see Table 2). The average K_2O value of the "paste group", recalculated without considering samples VD-6 and VD-8 is, in fact, equal to 2.64% while the RDS drops to 5%.

Na_2O and P_2O_5 show average values respectively equal to 1.15% and 0.35% by weight, with rather high RDS (25% and 37%). Also in this case, a correlation between chemical composition and mineralogy of the aplastic inclusions could be considered realistic. In fact, the unusual P_2O_5 concentration in this ceramic paste of samples VD-1 and VD-10, where clinopyroxene are particularly abundant could be explained considering the prismatic apatite inclusions that characterize larger clinopyroxene crystals. To be noted that P_2O_5 and TiO_2 are relatively less abundant in samples VD-6 and VD-8 (richer in sanidine crystal).

Equally interpretable in the light of the mineral-petrographic analyses are both the variability and the absolute value of the CaO concentrations. In this regard, all the analysed fragments show clear evidence of the presence of secondary calcite, both as an impregnation in the groundmass and/or as an external incrustation of variable thickness, which form during the long submergence of the *dolia* in the soil. The presence of a relevant quantity of calcium oxide not directly correlated to the initial composition of the ceramic paste should, therefore, be considered. Ceramic clay sources from continental deposits are generally much poorer in calcareous inclusions (microfossils) than clay sources from marine deposits.

Unfortunately, no comparison with the bulk chemistry of the ceramic pastes of the *dolia* found in S. Giovanni (Portoferraio, Elba Island) can be made, as Manca and co-authors (2016) did not carry out this analysis, but focused their research to the chemical analysis of the clinopyroxene with the electron microprobe. Comparison could only be made with the data recently reported by Thierrin-Michael and co-authors (2018) and concerning pottery production centres located along the Tyrrhenian coast of Italy, from Etruria to the Bay of Naples. However, as previously underlined, these data refer not to *dolia*, but rather to ceramic products that are quite different in terms of average size of the inclusions, i.e. wine amphorae (mostly type Dressel 1b and Dressel 2-4 produced from the 2nd to the 1st century B.C.). Fig. 8A compares the variation intervals and the average values of some major elements of the

Vagnari *dolia* with the corresponding data relating to the amphorae produced in Minturno and taken from Thierrin-Michael et al. (2018). In light of the above considerations, the slight shift in terms of average chemical composition could be likely interpreted as due to textural (aplastic inclusions are more abundant and with coarser size in *dolia*) and/or compositional differences (inclusions of sedimentary origin are relatively better represented in wine amphorae than the studied *dolia*) between the considered ceramic pastes.
Considering the trace elements (Tab. 4), it is possible to observe that for a part of them, in the *dolia* group, there are no significantly wide ranges of variation in concentration around the average values, as for Y, Sc, Cr, Co, Ni, Cu, Zn, Ga, As, Cs, Ta, Th and U. For another group of elements (Be, Ge, Mo, Ag, In, Sb, W, Tl, Bi), there is a generally very low concentration, comparable in the different samples, and relatively close to the instrumental lower detection limit. Samples VD-1 and VD-10, by contrast, differ in visibly higher concentrations in Ba and Sr than all other *dolia*, approximately 60% and 50% respectively. Instead, the VD-6 (mainly) and VD-8 samples are characterized by relatively low concentrations (about 30%) of V, Zr, Nb, Hf and rare earth elements, while the Rb is relatively more abundant (about 50%).
As for the major elements and even more so for the trace elements, the compositional comparison with the data relating to Roman wine amphorae (Thierrin-Michael et al., 2018) appears tricky. In fact, for trace elements, even the analysis procedure, in terms of precision and accuracy, can be more decisive. While our analyses were carried out by coupling ICP-OES and ICP-MS (after alkaline fusion and acid digestion), the analyses by Thierrin-Michael and co-authors were carried out by X-ray fluorescence spectrometry (XRFS). At any rate, in Fig. 8B it is possible to note an acceptable correspondence between the concentration values relating to the amphorae from Minturno and the *dolia* from Vagnari, specially in case of Rb, Zr, Y and Nb, while not negligible differences are recorded for Ba, Sr and some transition metals (Cr, Ni, Zn).

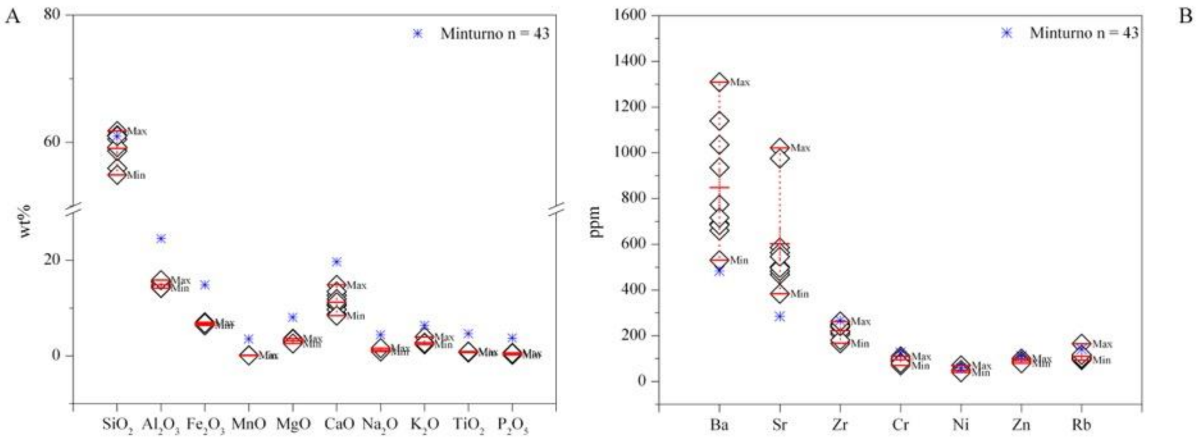

Figure 8. A) Variation intervals of major elements between dolia and ceramic products from Minturno; B) Variation intervals of trace elements between dolia and ceramic products from Minturno.

4.2.3 Chemical composition of clinopyroxenes

To obtain further confirmation and restrict as much as possible the potential area of production of the dolia, it was considered appropriate to perform chemical microanalysis on the clinopyroxene inclusions in the *dolia* pastes (major elements using EPMA and trace elements using ICP-MS with laser ablation). The obtained results suggest a satisfactory correspondence of the contents in rare earth elements with the clinopyroxene of the rocks characterizing the regions known as the Roman Magmatic Province and the Ernici-Roccamonfina Magmatic Province, where KS series consist of trachibasalts, latites, and trachytes, while ultrapotassic rocks and the HKS series mainly consist of leucite-bearing tephri-phonolites and leucitites (after Peccerillo 2005).

Major element analyses of representative clinopyroxenes (cpx) from the studied *dolia* are presented in Supplementary Material – Table S2. Small differences are observable between the cpx compositions of the analyzed *dolia*. The clinopyroxenes composing VD4, VD5, VD6 and VD7 ceramic paste display a relatively small range in composition, respectively Wo44-49 En34-50 Fs6–17 for VD4, Wo47-49 En36-43 Fs10–15 for VD5, Wo45-47 En35-43 Fs11–18 for VD6, Wo47-50 En29- 43 Fs10–22 for VD7, while sample VD8 slightly differs (Wo51-52 En32-37 Fs12-17). If plotted in the classification diagram of Morimoto et al. (1988) showed in Fig. 9, the measured compositions fall between the fields of diopsidic and salitic clinopyroxenes, showing a rather homogeneous SiO_2 abundance (from about 46 to about 49 wt. %) and magnesium number (Mg#) ranging from 0.70 to 0.77. In the same figure it is possible to note a good correspondence with the composition of the clinopyroxenes of the *dolia* found on the island of Elba and archaeometrically attributed by Manca et al. (2016) to a production centre located in the Roman Magmatic Province or in the adjacent Ercini-Roccamonfina Magmatic Province (Minturno).

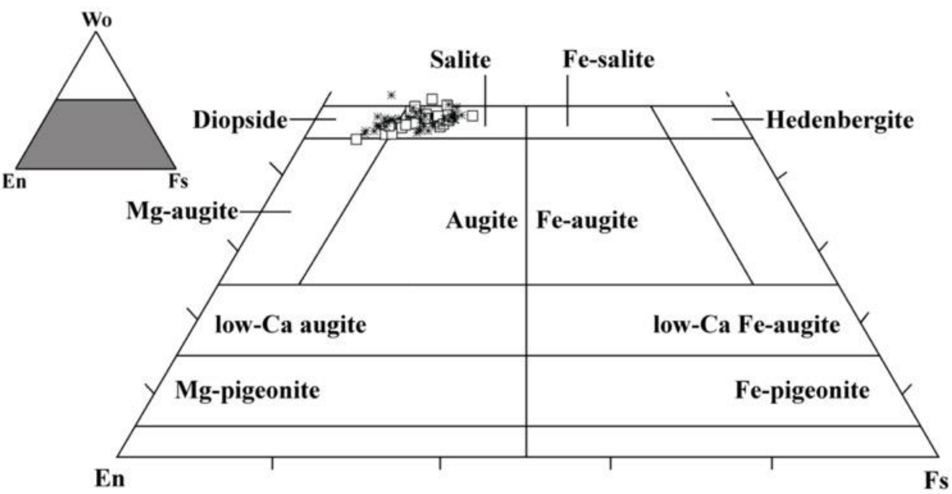

Figure 9. Plot of Cpx composition into the classification diagram for Ca–Mg–Fe pyroxenes (Morimoto et al., 1988): asterisk stands for Cpx composition from Manca et al., 2016.

Trace element abundance of the same clinopyroxenes (determined by laser ablation ICP-MS) are listed in Supplementary Material – Table S3. The elemental ratios of some selected trace elements in clinopyroxenes are renewed to be effective for fingerprinting magmatic provenance, because they are related to magma composition from equivalent tectonic settings as well as relevant for tectonic setting identification and geochemical sourcing (Peccerillo 2005). Specifically, ratios between elements Zr/Y vs Ce/Y and Ce/Lu vs Nd/Lu were used and compared with data available in the literature. They concern clinopyroxene analyses carried out from archaeological ceramic samples attributed to production centres located in the Roman Magmatic Province (Comodi et al. 2006; Belfiore et al. 2014; Gabriele et al. 2019) as well as pyroxenes of the volcanic rocks of the Magmatic Provinces most concerned in this study, i.e. Roman, Campanian and Ernici-Roccamonfina (Freda et al. 1997; Dallai et al. 2004; Comodi et al. 2006; Gaeta et al. 2006; Scarpelli et al. 2015). From the graphs in Figs. 10A-B, the acceptable correspondence between trace element ratios shown by the clinopyroxenes, which characterize the ceramic paste considered in this study, and those shown by the archaeological ceramic samples is quite evident. Similar trends (same trace elements ratios) can be also found by comparing the clinopyroxenes of this study with those present in the volcanic rocks of the above-mentioned Magmatic Provinces (Figs. 10C-D).

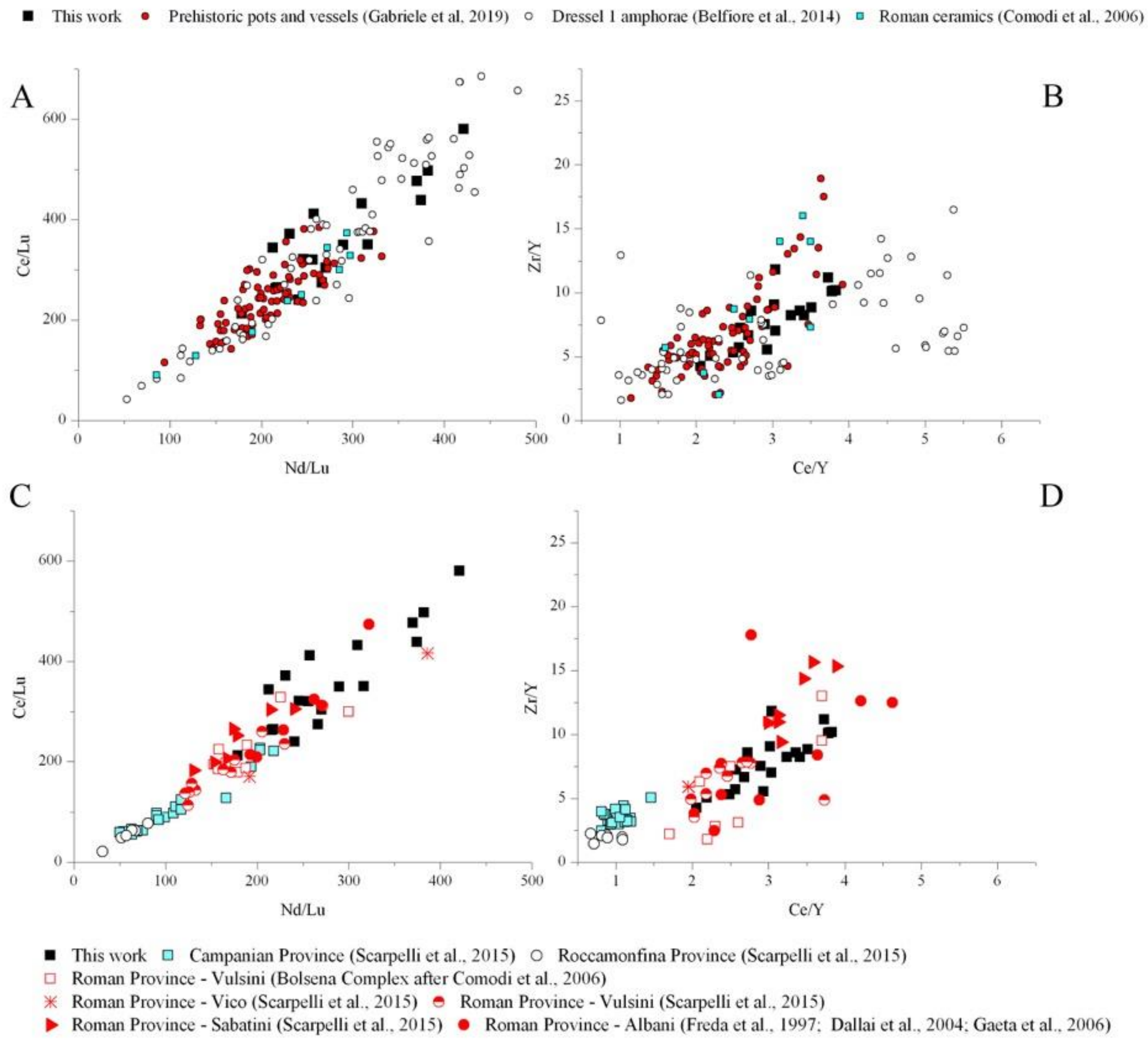

Figure 10. A-B) clinopyroxene trace elements ratios concerning the studied *dolia* and other archaeological ceramic samples; C-D) clinopyroxene trace elements ratios concerning the studied *dolia* and the volcanic rocks from some Italian Magmatic Provinces.

Conclusions

The analysis of tiles, misfired tiles, and raw clays at Vagnari shows that the natural resources needed for the production of roof tiles essential for the buildings of the central village on the Roman imperial estate took place in and around the village. Earlier discoveries of tile kilns at Vagnari further confirm this industrial activity which was important not only for Vagnari *vicus*, but probably also for other settlements in the region that were located on the property owned by the Emperor since the early 1st century A.D. The *dolia*, on the other hand, were made of clay that came from the Tyrrhenian coast of Latium and Campania, from the Roman Magmatic Province (with Rome at its centre) or the Ernici Roccamonfina Magmatic Province (with Minturno as a key site). This is of particular importance for an understanding of the Roman economy, the mobility of manufactured goods, and supply networks. Normally, the kilns and manufacturing centres for *dolia* were located at or near the sites at which wine was produced, as at Giancola near Brindisi (Puglia), which is not very far from Vagnari (Manacorda and Pallecchi 2012). But the Emperor as landowner of the Vagnari estate did not procure the equipment for his 2nd-century winery locally from these or other private providers. In Latium, especially around the capital city of Rome, heavy ceramics, including *dolia*, were manufactured in vast quantities in production centres in private ownership, many of them gradually being transferred to imperial ownership (Lazzeretti and Pallecchi 2005; Gliozzo and Filippi 2005; Lo Cascio 2005). The estates in the hinterland of the Roman town of *Minturnae*, modern Minturno, on the border between Latium and Campania, also were particularly active in the production of wines, the *dolia* for winery storage, and the very large *dolia* for bulk transport of wine by ship in the western Mediterranean, although it is unknown whether any of the properties were in imperial possession (Johnson 1933: 126-128; Lazzeretti 1998; Bellini and Trigona 2013; Gregori and Nonnis 2013; Heslin 2011: 165-166). The workshops around Rome or around Minturno are the likely source of the Vagnari *dolia*, although Minturno is a better match for the fabric of the *dolia*. It is likely that the *dolia* destined for Vagnari were shipped by sea around the toe of the Italian peninsula, perhaps to the Adriatic coast or up the rivers draining into the Ionian Gulf, and then brought overland to Vagnari. Why this seemingly inconvenient provision of equipment from the other side of Italy took place is unclear, but distance and expense clearly played little role in the Emperor's decision to establish a winery at Vagnari.

Acknowledgements

We are grateful to the British Academy for the financial support that made this project possible (Grant No. SG162763, Apulian Wine and Adriatic Trade in the Early Roman Empire. A Study of Dolia as a Physical Medium for the Production and Long-Range Transport of Eastern Italian Vintages, 2017-2018). We thank the Soprintendenza per i Beni Archeologici della Puglia for the excavation permit and for permission to sample the ceramics for analysis. We also thank Alastair Small (University of Edinburgh), Irene de Luis (Sheffield), and Veronica Ferrari and Giuseppe Ceraudo (Università del Salento) for photos and drawings.

References

Aoyagi, M., De Simone, A., De Simone, G.F., 2018. The "Villa of Augustus" at Somma Vesuviana, in: A. Marzano (Ed.), The Roman Villa in the Mediterranean Basin. Late Republic to Late Antiquity. Cambridge: Cambridge University Press, 141-156.

Azzaroli, A., Perno, U., Radina, B., 1968. Note illustrative della Carta Geologica d'Italia - Foglio Geologico 188 "Gravina in Puglia", Servizio Geologico d'Italia. Rome: Istituto Superiore per la Protezione e la Ricerca Ambientale.

Belfiore, C.M., La Russa, M.F., Barca, D., Galli, G., Pezzino, A., Ruffolo, S.A., Viccaro, M., Fichera, G.V., 2014. A trace element study for the provenance attribution of ceramic artefacts: the case of Dressel 1 amphorae from a late-Republican ship. J. Archaeol. Sci., 43, 91-104.

Bellini, G.R. and Trigona, S.L., 2013. Minturnae e il Garigliano: l'attività di ricerche del 2012. Lazio e Sabina, 10, 265-272.

Bonifacio, G., 2004. In Stabiano. Exploring the Ancient Seaside villas of the Roman Elite, in: Nicola Langobardi (Ed.), Castellamare di Stabia.

Carroll, M., 2016. Vagnari. Is this the winery of Rome's greatest landowner? Curr. World Archaeol., 76, 30-33.

Carroll, M., 2019. Preliminary Report on the University of Sheffield Excavations in the vicus of the Roman Imperial Estate at Vagnari, Puglia, 2012-2018. FastiOnline FOLD&R 2019-432 www.fastionline.org/docs/FOLDER-it-2019-431.pdf

Cau Ontiveros, M.A., Day, P.M., Montana, G., 2002. Secondary calcite in archaeological ceramics: evaluation of alteration and contamination processes by thin section study, in V. Kilikoglou, A. Hein, Y. Maniatis (Eds.), Modern trends in ancient ceramics (British Archaeological Reports, International Series 1011). Oxford: Archaeopress, 9-18.

Celuzza, M.G., 1985. *Opus doliare*, in: A. Carandini (Ed.), Settefinestre. Una villa schiavistica nell'Etruria romana, Vol. 3, La villa e i suoi reperti. Modena: Edizioni Panini, 59-61.

Comodi, P., Nazzareni, S., Perugini, D., Bergamini, M., 2006. Technology and provenance of roman ceramics from Scoppieto, Italy: a mineralogical and petrological study. Per. Mineralogia, 75(2-3), 95-112.

Dallai, L., Freda, C., Gaeta, M., 2004. Oxygen isotope geochemistry of pyroclastic clinopyroxene monitors carbonate contributions to Roman-type ultrapotassic magmas. Contributions to Mineralogy and Petrology, 148(2), 247-263.

De Caro, S., 1994. La Villa Rustica in Localita Villa Regina a Boscoreale, in: Giorgio Bretschneider Editore. Roma.

Dell'Amico, P., Pallarés, F., 2005. Il relitto di Diano Marina e le navi a dolia: nuove considerazioni, in: T. Cortis and T. Gambin (Eds.), De Triremibus. Festschrift in Honour of Joseph Muscat. San Gwann: Publishers Enterprises Group, 67-114.

Depalo, M.R., 2017. Piana San Felice: un sito archeologico pluristratificato nel territorio di Gravina in Puglia, in: L. Cossalter and M.R. Depalo (Eds.), Il paesaggio storico ricostruito. L'insediamento di Piana San Felice a Gravina in Puglia. Bari: Edipuglia, 25-38.

Di Pierro, M., 1981. I caratteri composizionali delle argille pleistoceniche della zona di Miglionico (MT). Rendiconti della Società Italiana di Mineralogia e Petrografia, 37(1), 229-240.

Freda, C., Gaeta, M., Palladino, D.M., Trigila, R., 1997. The Villa Senni Eruption (Alban Hills, central Italy): the role of H_2O and CO_2 on the magma chamber evolution and on the eruptive scenario. J. Volcanol. Geotherm. Res., 78A, 103-120.

Gabriele, M., Convertini, F., Verati, C., Gratuze, B., Jacomet, S., Boschian, G., Durrenmath, G., Guilaine, J., Lardeaux, J.M., Gomart L., Manen, C., Binder, D., 2019. Long-distance mobility in the North-Western Mediterranean during the Neolithic transition using high resolution pottery sourcing. J. Archaeol. Sci.: Rep., 28, 102050.

Gaeta, M., Freda, C., Christensen, J.N., Dallai, L., Marra, F., Karner, D.B., Scarlato, P., 2006. Time-dependent geochemistry of clinopyroxene from the Alban Hills (central Italy): clues to the source and evolution of ultrapotassic magmas. Lithos, 86, 330-346.

Gao, S., Liu, X., Yuan H., Hattendorf, B., Günther, D., Chen, L., Hu, S., 2002. Determination of forty two major and trace elements in USGS and NIST SRM glasses by laser ablation–

inductively coupled plasma-mass spectrometry. Geostand. Newsl., 26(2), 181-196.

Gliozzo, E., 2020. Ceramic technology. How to reconstruct the firing process. Archaeol. Anthropol. Sci., 12, 260 (https://doi.org/10.1007/s12520-020-01133-y).

Gliozzo, E., Filippi, G., 2005. Archeologia e archeometria della produzione doliare bollata 'urbana' ulteriori dati e riflessioni, in: C. Bruun (Ed.), Interpretare i bolli laterizi di Roma e della Valle del Tevere: Produzione, storia economica e topografia. Atti del Convengno all'Ecole Francaise de Rome e all'Institutum Romanum Finlandiae, 31 marzo e 1 aprile 2000 (Acta Instituti Romani Finlandiae 32). Rome: Institutum Romanum Finlandiae, 229-247.

Gliozzo, E., Turchiano, M., Fantozzi, P.L., Romano, A.V., 2018. Georesources for ceramic production and communication pathways: the exchange network and the scale of chemical representative differences. Appl. Clay Sci., 161, 242-255.

Gregori, G.L., Nonnis, D., 2013. Dal Liris al Mediterraneo. Rapporto dell'epigrafia repubblicana alla storia del porto di Minturnae, in: G. Olcese (Ed.), Immensa Aequora. Workshop. Richerche archeologiche, archeometriche e informatiche per la ricostruzione dell'economia e dei commerci nel bacino occidentale del Meterraneo (meta IV sec. a.C. – I sec. d.C.). Atti del Convegno Roma 24-26 gennaio 2011. Rome: Edizioni Quasar, 163-177.

Hein, A., Kilikoglou, V., 2020. Ceramic raw materials: how to recognize them and locate the supply basins: chemistry. Archaeol. Anthropol. Sci., 12, 180 (https://doi.org/10.1007/s12520-020-01129-8).

Heslin, K., 2011. *Dolia* Shipwrecks and the wine trade in the Roman Mediterranean, in: D. Robinson and A. Wilson (Eds.), Maritime Archaeology and Ancient Trade in the Mediterranean: 157-168. Oxford: Oxford Centre for Maritime Archaeology.

Johnson, J., 1933. Excavations at Minturnae, Vol. 2. The Inscriptions. Part 1: Republican Magistri. Rome: The International Mediterranean Research Association.

Lambrugo, C., Pace, A., 2017. Il "Complesso Alfa", fasi di vita e rituali di abbandono, in: M. Castoldi (Ed.), I Peuceti a Jazzo Fornasiello. Scavi archeologici a Jazzo Fornasiello, Gravina in Puglia. Milano: Edizioni Et, 31-40.

Lazzeretti A., 1998. Un *dolium* di *M'. Codonius* e i *dolia* prodotti a Minturno rinvenuti a terra. Bollettino della Commissione Archeologica Comunale di Roma, 99, 338-346.

Lazzeretti, A., Pallecchi, S., 2005. Le figlinae 'polivalenti': la produzione di dolia e di mortaria bollati, in: C. Bruun (Ed.) Interpretare i bolli laterizi di Roma e della Valle del Tevere: Produzione, storia economica e topografia. Atti del Convegno all'Ecole Francaise de Rome e all'Institutum Romanum Finlandiae, 31 marzo e 1 aprile 2000 (Acta Instituti Romani Finlandiae 32). Rome: Institutum Romanum Finlandiae, 213-227.

Lo Cascio, E., 2005. La concentrazione delle figlinae nella proprieta imperial (II-IV sec.), in C. Bruun (Ed.), Interpretare i bolli laterizi di Roma e della Valle del Tevere: Produzione, storia economica e topografia. Atti del Convegno all'Ecole Francaise de Rome e all'Institutum Romanum Finlandiae, 31 marzo e 1 aprile 2000 (Acta Instituti Romani Finlandiae 32). Rome: Institutum Romanum Finlandiae, 95-102.

Manca, R., Pagliantini, L., Pecchioni, E., Santo, A.P., Cambi, F., Chiarantini, L., Corretti, A., Costagliola, P., Orlando, A., Benvenuti, M., 2016. The island of Elba (Tuscany, Italy) at the crossroads of ancient trade routes: an archaeometric investigation of dolia defossa from the archaeological site of San Giovanni. Mineral. and Petrol., 110, 693-711.

Maritan, L., 2020. Ceramic abandonment. How to recognise post-depositional transformations. Archaeol. Anthropol. Sci., 12, 199 (https://doi.org/10.1007/s12520-020-01141-y).

Matthews, A.J., Woods, A.J., Oliver, C., 1991. Spots before your eyes: new comparison charts for visual percentage estimation in archaeological material, in: A.P. Middleton and I.C. Freestone (Eds.) Recent developments in ceramic petrology (British Museum Occasional Paper 81). London: The British Museum, 211-263.

Montana, G., 2020. Ceramic raw materials: how to recognize them and locate the supply basins-mineralogy, petrography. Archaeol. Anthropol. Sci., 12, 175 (https://doi.org/10.1007/s12520-020-01130-1).

Morimoto, N., Fabries, J., Ferguson, A.K., Ginzburg, I.V., Ross, M., Seifert, F.A., Zussman, J., Aoko, K., Gottardi, G., 1988. Nomenclature of pyroxenes. Am. Mineral., 73, 1123-1133.

Pearce, N.J.G., Perkins, W.T., Westgate, J.A., Gorton, M.P., Jackson, S.E., Neal, C.R., Chenery, S.P., 1997. A compilation of new and published major and trace element data for NIST SRM 610 and NIST SRM 612 glass reference materials. Geostand. Newsl., 21, 115-144.

Peccerillo, A., 2005. Plio-Quaternary volcanism in Italy. Berlin: Springer.

Pieri, P., Sabato, L., Spalluto, L., Tropeano, M., 2012. Note illustrative alla Carta Geologica d'Italia, F. 248 (Bari), Servizio Geologico d'Italia. Rome: Istituto Superiore per la Protezione e la Ricerca Ambientale.

Pietropaolo, L., 1998. La villa, in: G. Volpe (Ed.), San Giusto. La villa, le ecclesiae. Bari: Edipuglia, 49-66.

Scarpelli, R., De Francesco, A.M., Gaeta, M., Cottica, D., Toniolo, L., 2015. The provenance of the Pompeii cooking wares: Insights from LA–ICP-MS trace element analyses. Microchem. J., 119, 93-101.

Sciallano, M., Marlier, S., 2008. L'épave à dolia de l'île de La Giraglia (Haute-Corse). Archaeonautica, 15, 113-151.

Small, A.M., 1992. Botromagno: an introduction, in: A.M. Small (Ed), Gravina. An Iron Age and Republican Settlement in Apulia, Vol. 1, The Site. London: British School at Rome, 1-18.

Small, A.M., 2001. Changes in the pattern of settlement and land use around Gravina and Monte Irsi (4th century BC – 6th century AD), in: E. Lo Cascio and A. Storchi Marino (Eds.), Modalità insediative e strutture agrarie nell'Italia meridionale in età romana. Bari: Edipuglia, 35-53.

Small, A.M., 2011. Introduction, in: A. M. Small (Ed.), Vagnari. Il villaggio, l'artigianato, la proprietà imperiale. Bari: Edipuglia, 11-36.

Small, A.M., Volterra, V., Hancock, R.G.V., 2003. New evidence from tile-stamps for imperial properties near Gravina, and the topography of imperial estates in SE Italy. J. Rom. Archaeol.,16, 178-199.

Small, C., 2011. The Surface Collection, in: A. M. Small (Ed.), Vagnari. Il villaggio, l'artigianato, la proprietà imperiale. Bari: Edipuglia, 53-72.

Thierrin-Michael, G., Tretola Martinez, D.C., Serneels, V., 2018. Assessment of the amphora spectrum in a rural late La Tène settlement at Reinach-Nord, Basel region, Switzerland. J. Archaeol. Sci.: Rep., 21, 1055-1063.

Table 1. List of analyzed samples.

Sample code	Typology		Analytical methods
VW-1	Kiln waste		OM, ICP-MS/OES (bulk)
VW-2	Kiln waste		
VT-1	Roof tile		OM, ICP-MS/OES (bulk)
VT-2	Roof tile		
VT-3	Roof tile		
VT-4	Roof tile		
VT-5	Roof tile		
VT-6	Roof tile		
VT-7	Roof tile		
VT-8	Roof tile		
VT-9	Roof tile		
VT-10	Roof tile		
VT-11	Roof tile		
VT-12	Roof tile		
VD-1	Dolium		OM, ICP-MS/OES (bulk) LA-ICP-MS (clinopyroxenes)
VD-2	Dolium		
VD-3	Dolium		
VD-4	Dolium		
VD-5	Dolium		
VD-6	Dolium		
VD-7	Dolium		
VD-8	Dolium		
VD-9	Dolium		
VD-10	Dolium		
Raw clays	**Location of sampling point (coordinates)**	**Firing Temperature (°C)**	**Munsell Color (before/after firing)**
VC-1	Lat: 40,833831 Lon: 16,271315	raw paste	light greenish grey 8/1 10Y
VC-1.1		700 °C	reddish yellow 7/6 5YR
VC-1.2		800 °C	reddish yellow 6/8 5YR
VC-1.3		900 °C	light red 7/8 2.5 YR
VC-2	Lat: 40,835975 Lon: 16,2740238	raw paste	light bluish grey 8/1 5PB
VC-2.1		700 °C	reddish yellow 6/6 5YR
VC-2.2		800 °C	reddish yellow 6/8 5YR
VC-2.3		900 °C	reddish yellow 6/8 5YR

Table 2. Major and trace elements concentrations relative to the local tiles (VW and VT-series) and to the clayey raw materials (VC). LOI normalized chemical compositions.

Oxides (%)	VW-1	VW-2	VT-1	VT-2	VT-3	VT-4	VT-5	VT-6	VT-7	VT-8	VT-9	VT-10	VT-11	VT-12	MEAN	ST. DEV	RSD (%)	VC-1	VC-2	MEAN
SiO_2	56.09	55.21	57.42	55.06	57.71	56.24	59.28	57.90	56.89	56.90	56.04	56.84	56.38	55.55	**56.68**	**1.15**	**2.02**	55.25	57.50	**56.37**
Al_2O_3	16.17	15.88	15.77	14.46	13.42	15.79	15.39	15.73	15.41	15.36	15.56	15.27	15.69	15.24	**15.37**	**0.69**	**4.49**	16.00	13.77	**14.88**
Fe_2O_3(T)	6.06	6.05	6.11	5.67	5.16	6.23	6.02	5.84	5.83	5.90	5.90	5.88	6.04	5.99	**5.91**	**0.26**	**4.34**	6.42	5.38	**5.90**
MnO	0.09	0.09	0.10	0.10	0.10	0.10	0.13	0.10	0.10	0.10	0.11	0.10	0.10	0.11	**0.10**	**0.01**	**9.12**	0.10	0.10	**0.10**
MgO	2.86	2.99	2.62	3.30	1.94	2.64	2.01	2.46	2.32	2.67	2.34	3.10	2.77	2.87	**2.63**	**0.39**	**14.85**	2.90	1.69	**2.30**
CaO	13.65	14.95	12.82	17.26	17.06	13.96	12.48	12.97	14.74	14.09	15.43	14.25	13.93	15.44	**14.50**	**1.44**	**9.92**	14.59	17.51	**16.05**
Na_2O	1.24	1.08	1.17	0.85	1.18	1.16	0.99	1.11	1.00	1.14	0.80	0.89	1.17	1.08	**1.06**	**0.14**	**12.87**	1.10	0.94	**1.02**
K_2O	2.90	2.83	3.02	2.42	2.57	2.94	2.74	2.89	2.73	2.93	2.92	2.75	2.92	2.74	**2.81**	**0.16**	**5.79**	2.75	2.30	**2.53**
TiO_2	0.75	0.73	0.75	0.68	0.62	0.73	0.71	0.72	0.71	0.71	0.71	0.70	0.74	0.71	**0.71**	**0.03**	**4.52**	0.74	0.65	**0.70**
P_2O_5	0.20	0.19	0.22	0.21	0.25	0.21	0.26	0.28	0.27	0.21	0.19	0.21	0.27	0.28	**0.23**	**0.03**	**14.14**	0.16	0.15	**0.15**
Element (ppm)	**VW-1**	**VW-2**	**VT-1**	**VT-2**	**VT-3**	**VT-4**	**VT-5**	**VT-6**	**VT-7**	**VT-8**	**VT-9**	**VT-10**	**VT-11**	**VT-12**	**MEAN**	**ST. DEV**	**RSD (%)**	**VC-1**	**VC-2**	**MEAN**
Sc	14	14	14	12	11	14	13	13	12	13	12	12	14	13	**13**	**1**	**8**	12	10	**11**
Be	3	3	3	2	2	3	2	3	2	2	2	2	3	3	**3**	**1**	**21**	2	2	**2**
V	134	133	106	99	99	113	109	108	108	104	111	106	112	107	**111**	**11**	**10**	117	96	**107**
Ba	340	346	447	524	602	380	553	484	525	411	597	701	407	328	**475**	**114**	**24**	285	283	**284**
Sr	329	403	325	394	310	321	264	298	270	314	280	244	326	336	**315**	**45**	**14**	309	268	**289**
Y	25	25	23	21	19	23	21	23	21	22	21	19	24	23	**22**	**2**	**9**	24	22	**23**
Zr	142	145	141	126	136	140	147	137	123	138	128	119	133	134	**135**	**8**	**6**	127	140	**134**
Cr	110	120	100	100	90	100	100	90	100	100	90	90	110	110	**101**	**9**	**9**	90	80	**85**
Co	12	12	12	10	9	12	13	11	10	12	11	11	12	12	**11**	**1**	**10**	10	9	**10**
Ni	50	50	50	50	40	60	50	50	50	50	50	50	60	50	**51**	**5**	**9**	50	40	**45**

Cu	30	30	30	30	20	30	30	20	30	30	30	20	30	30	**28**	**4**	**15**	20	20	**20**
Zn	100	110	100	90	80	100	90	90	90	100	90	90	100	140	**98**	**14**	**15**	90	70	**80**
Ga	21	21	20	18	15	20	19	19	18	19	18	17	21	20	**19**	**2**	**9**	17	15	**16**
Ge	2	2	2	1	1	2	2	2	1	1	1	1	2	1	**2**	**1**	**35**	1	1	**1**
As	6	10	11	9	9	9	10	11	8	9	8	10	10	10	**9**	**1**	**14**	8	9	**9**
Rb	121	122	117	64	88	112	95	113	92	112	97	89	106	109	**103**	**16**	**16**	107	87	**97**
Nb	16	17	16	15	13	17	16	16	15	16	16	15	17	17	**16**	**1**	**7**	14	12	**13**
Mo	< 2	< 2	< 2	< 2	4	< 2	< 2	< 2	< 2	< 2	< 2	< 2	< 2	< 2	**4**		**0**	< 2	< 2	
Ag	< 0.5	< 0.5	< 0.5	< 0.5	< 0.5	< 0.5	< 0.5	< 0.5	< 0.5	< 0.5	< 0.5	< 0.5	< 0.5	< 0.5				< 0.5	< 0.5	
In	< 0.2	< 0.2	< 0.2	< 0.2	< 0.2	< 0.2	< 0.2	< 0.2	< 0.2	< 0.2	< 0.2	< 0.2	< 0.2	< 0.2				< 0.2	< 0.2	
Sn	3	3	3	3	3	3	3	3	3	3	3	3	4	3	**3**	**0**	**9**	3	2	**3**
Sb	0.6	0.5	< 0.5	< 0.5	< 0.5	< 0.5	0.5	0.8	< 0.5	< 0.5	< 0.5	0.5	< 0.5	0.5	**1**	**0**	**21**	< 0.5	< 0.5	
Cs	6.5	6.8	6	2.6	4.2	6	4.7	6	5.1	5.8	4.6	4.1	5.8	6	**5**	**1**	**22**	5.8	4.4	**5**
La	35.8	39.2	35.5	32.5	28	35.6	35.4	34.5	31.1	34.5	34.3	30.3	36	35.5	**34**	**3**	**8**	29.6	27.3	**28**
Ce	69.9	75.7	69.4	63.3	55.1	70.2	69.1	67.6	60.9	67.7	66.7	59.3	70.1	69.4	**67**	**5**	**8**	58.1	56.5	**57**
Pr	8.22	8.68	8.06	7.28	6.35	8.06	7.77	7.77	7.06	7.8	7.66	6.84	8.07	7.89	**8**	**1**	**8**	6.78	6.2	**6**
Nd	30.7	32.7	30.1	27.3	24.2	29.8	28.8	28.3	25.6	28.4	27.9	25.5	30.1	29.4	**28**	**2**	**8**	24.4	22.8	**24**
Sm	6.3	6.5	6.1	5.6	4.9	6.2	5.7	6	5.2	5.8	5.7	5.1	6.1	5.9	**6**	**0**	**8**	4.9	4.8	**5**
Eu	1.24	1.36	1.29	1.1	1.07	1.28	1.27	1.2	1.07	1.18	1.14	1.06	1.31	1.24	**1**	**0**	**8**	1.06	0.97	**1**
Gd	5.1	5.5	5.2	4.6	4.3	5	5.1	4.9	4.3	5	4.5	4.4	5.1	5	**5**	**0**	**8**	4.3	3.9	**4**
Tb	0.8	0.8	0.8	0.7	0.7	0.8	0.8	0.8	0.7	0.8	0.7	0.6	0.8	0.8	**1**	**0**	**9**	0.6	0.7	**1**
Dy	4.9	4.9	4.8	4.3	4	4.7	4.6	4.6	4.1	4.8	4.3	3.9	4.8	4.5	**5**	**0**	**8**	4	3.8	**4**
Ho	0.9	0.9	0.9	0.8	0.8	0.9	0.9	0.9	0.8	0.9	0.8	0.7	0.9	0.9	**1**	**0**	**8**	0.8	0.7	**1**
Er	2.6	2.8	2.7	2.5	2.2	2.6	2.6	2.5	2.2	2.6	2.5	2.2	2.7	2.6	**3**	**0**	**8**	2.2	2	**2**
Tm	0.4	0.4	0.38	0.34	0.33	0.36	0.38	0.36	0.32	0.38	0.34	0.31	0.4	0.35	**0**	**0**	**8**	0.32	0.31	**0**

Yb	2.6	2.7	2.5	2.3	2.1	2.5	2.5	2.5	2.3	2.6	2.2	2.1	2.7	2.5	**2**	**0**	**8**	2.1	2	**2**
Lu	0.36	0.39	0.39	0.35	0.32	0.39	0.36	0.37	0.34	0.38	0.31	0.34	0.37	0.36	**0**	**0**	**7**	0.32	0.31	**0**
Hf	4.3	4.9	4.5	4.1	4.3	4.6	4.6	4.2	4	4.4	4.1	3.8	4.4	4.4	**4**	**0**	**6**	3.8	4.3	**4**
Ta	1.3	1.3	1.3	1.1	1	1.3	1.2	1.2	1.1	1.2	1.1	1.1	1.1	1.3	**1**	**0**	**9**	1	0.9	**1**
W	1	1	1	< 1	10	9	< 1	1	1	1	1	1	1	< 1	**3**	**3**	**135**	1	1	**1**
Tl	< 0.1	< 0.1	0.1	0.1	0.3	0.1	0.5	0.5	0.5	0.3	0.5	0.4	0.2	0.1	**0**	**0**	**59**	0.4	0.3	**0**
Pb	8	13	17	10	15	16	16	18	16	17	17	14	16	20	**15**	**3**	**21**	15	12	**14**
Bi	< 0.4	< 0.4	< 0.4	< 0.4	< 0.4	< 0.4	< 0.4	< 0.4	< 0.4	< 0.4	< 0.4	< 0.4	< 0.4	< 0.4				< 0.4	< 0.4	
Th	11.6	12	11.5	10.1	8.9	11.3	10.5	11.2	9.8	10.9	10.3	9.5	11.3	11.1	**11**	**1**	**8**	9.7	8.4	**9**
U	2.8	3	3.3	2.6	2.9	2.7	2.3	3.3	2.3	3.1	3.4	2.4	2.7	2.7	**3**	**0**	**13**	2.6	2.2	**2**

Table 3. Major elements concentrations relative to the *dolia* (VD). LOI normalized chemical compositions.

Sample code	SiO_2	Al_2O_3	Fe_2O_3(T)	MnO	MgO	CaO	Na_2O	K_2O	TiO_2	P_2O_5
VD-1	61.38	14.69	6.69	0.11	2.60	8.68	1.64	2.73	0.86	0.64
VD-2	58.69	14.17	6.54	0.14	3.28	12.60	0.92	2.55	0.81	0.26
VD-3	55.75	14.28	6.43	0.14	3.60	14.73	1.26	2.39	0.84	0.42
VD-4	60.32	14.20	6.63	0.13	3.48	10.52	0.92	2.63	0.89	0.28
VD-5	60.85	14.68	6.70	0.12	3.00	9.70	1.01	2.71	0.83	0.35
VD-6	54.75	15.61	6.76	0.11	3.20	13.43	1.21	3.96	0.70	0.24
VD-7	58.84	14.86	7.00	0.13	3.51	10.78	0.96	2.71	0.92	0.28
VD-8	58.50	15.41	6.39	0.13	2.85	11.89	1.02	2.95	0.79	0.23
VD-9	59.03	14.23	7.00	0.17	3.46	11.21	0.91	2.74	0.90	0.34
VD-10	60.66	15.80	6.80	0.11	2.59	8.39	1.62	2.69	0.87	0.49
MEAN	**58.88**	**14.79**	**6.69**	**0.13**	**3.16**	**11.19**	**1.15**	**2.81**	**0.84**	**0.35**
ST. DEV	**2.17**	**0.62**	**0.21**	**0.02**	**0.38**	**2.03**	**0.28**	**0.43**	**0.07**	**0.13**
RSD (%)	**3.69**	**4.16**	**3.14**	**13.95**	**11.97**	**18.11**	**24.51**	**15.39**	**7.76**	**36.68**

Table 4. Trace elements concentrations relative to the *dolia* (VD).

Element (ppm)	VD-1	VD-2	VD-3	VD-4	VD-5	VD-6	VD-7	VD-8	VD-9	VD-10
Sc	12	17	15	17	15	15	18	14	17	12
Be	3	3	3	3	2	3	3	3	2	3
V	128	133	135	133	137	120	136	105	132	120
Ba	1309	660	773	689	684	936	716	531	835	1140
Sr	1022	468	586	482	502	563	497	384	546	975
Y	33	30	29	30	29	26	33	29	33	35
Zr	251	215	207	238	217	167	244	181	242	263
Cr	70	100	90	110	100	110	110	90	100	80
Co	13	14	15	15	13	14	17	15	16	14
Ni	40	50	50	50	40	70	50	50	50	40
Cu	20	20	30	20	20	20	20	30	20	20
Zn	90	90	90	90	90	100	90	100	90	80
Ga	22	20	19	20	20	20	21	20	20	23
Ge	2	2	2	2	2	1	2	2	2	2
As	9	9	11	9	8	11	8	8	5	12
Rb	113	98	94	99	100	165	105	142	102	117
Nb	36	20	26	21	19	15	22	18	21	37
Mo	< 2	< 2	2	< 2	< 2	< 2	< 2	< 2	< 2	< 2
Ag	< 0.5	< 0.5	< 0.5	< 0.5	< 0.5	< 0.5	< 0.5	< 0.5	< 0.5	< 0.5
In	< 0.2	< 0.2	< 0.2	< 0.2	< 0.2	< 0.2	< 0.2	< 0.2	< 0.2	< 0.2
Sn	4	4	3	4	17	4	4	4	4	4
Sb	0,5	0,6	0,5	< 0.5	0,7	0,8	< 0.5	< 0.5	< 0.5	0,7
Cs	6,5	5	5,3	4,9	4,7	9,6	5,3	5,6	5,2	6,7
La	104	58,6	70,9	59,1	54	47	64,3	44,1	66,1	104
Ce	194	118	137	121	107	96	130	87	133	192
Pr	21,2	14,2	15,7	14,3	12,6	10,5	15,5	10,1	15,9	21
Nd	75,5	53,8	58,3	55,3	47,6	38,1	59,9	38,1	60,3	75,3
Sm	13,6	10,6	11	10,6	9,5	7,3	11,7	7,9	11,4	13,7
Eu	3,05	2,29	2,37	2,32	2,01	1,48	2,56	1,6	2,58	3,01
Gd	9,9	8,3	8,3	8,3	7,2	5,4	9,1	6,4	9,2	9,8
Tb	1,4	1,1	1,2	1,2	1	0,8	1,3	1	1,3	1,4
Dy	7,2	6,4	6,2	6,5	5,6	4,7	7	5,4	6,9	7,3
Ho	1,3	1,2	1,1	1,1	1	0,9	1,3	1	1,2	1,3
Er	3,3	3,1	3	3,2	2,9	2,4	3,4	2,9	3,3	3,4
Tm	0,47	0,43	0,41	0,43	0,4	0,35	0,48	0,41	0,44	0,45
Yb	3	2,7	2,8	2,7	2,7	2,4	2,9	2,6	3	3

Lu	0,42	0,41	0,37	0,42	0,39	0,38	0,42	0,42	0,41	0,44
Hf	7,3	6,5	6,1	6,9	6,8	5	7,2	5,2	7,6	7,6
Ta	2,4	1,4	1,6	1,5	1,2	1,2	1,6	1,3	1,6	2,3
W	1	1	1	1	2	2	1	1	1	1
Tl	0,3	0,5	0,4	0,5	0,5	1	0,5	0,5	0,5	0,3
Pb	34	19	26	20	1640	53	21	21	27	35
Bi	< 0.4	< 0.4	< 0.4	< 0.4	< 0.4	< 0.4	< 0.4	< 0.4	< 0.4	< 0.4
Th	27,9	15,1	18,7	15,2	14,2	18,3	16,4	13,4	16,7	27,9
U	4,8	3,8	3,7	3,8	4,4	4,4	4	3,5	4,3	4,6

Table S1 – Supplementary Material. Schematic description of the compositional and textural features of the studied samples.

Sample code	Aplastic inclusions								Groundmass			Secondary calcite
	Distribution	Sorting	Aplastic grain size distribution	MGS (mm)	Packing (%)	Monomineralic grains	Rock fragments	Microfossils (M) Limestones (L) Micritic clots (mc)	Clay Lumps	Optical activity	Porosity	
VW-1	Moderately homogeneous	Serial	coarse silt – medium sand	0.5	5-10%	Qtz (+++), Qtz pol (++), Ms (++/+), Kfs (+), Pl (r), Cpx (r)	acid crystalline rocks (r), chert (r)	-	++	inactive	vugs, cast	++
VW-2	Heterogeneous	Serial	coarse silt – fine sand	0.2	5%	Qtz (+++), Qtz pol (++), Ms (++/+), Kfs (+), Pl (r), Cpx (r)	acid crystalline rocks (r), chert (r)	-	++	inactive	vugs, cast	++
VT-1	Moderately homogeneous	Serial	coarse silt – fine sand	0.3	5-10%	Qtz (+++), Qtz pol (++), Ms (+++), Kfs (+), Pl (r), Cpx (r)	acid crystalline rocks (+)	+++ (mc)	++	inactive	cast	++
VT-2	Heterogeneous	Serial	coarse silt – very fine sand	0.2	5-8%	Qtz (+++), Qtz pol (++), Ms (+++), Kfs (+), Pl (r), Cpx (r)	acid crystalline rocks (+)	+++ (M)	++	inactive	cast	+++
VT-3	Moderately homogeneous	Serial	coarse silt - coarse sand (sporadic)	0.8	10-15%	Qtz (+++), Qtz pol (++), Ms (++), Kfs (+), Pl (+)	acid crystalline rocks (r), chert (++), sandstones (+)	+++ (M)	++	active	vugs, cast	+
VT-4	Moderately homogeneous	Serial	coarse silt – fine sand	0.25	5-8%	Qtz (+++), Qtz pol (++), Ms (++), Kfs (+), Pl (+)	chert (+)	++ (mc)	++	active	vugs, cast	+/++
VT-5	Moderately homogeneous	Serial	coarse silt - medium sand	0.5	10%	Qtz (+++), Qtz pol (++), Ms (++), Kfs (+), Pl (+)	chert (++), sandstones (+)	++ (mc)	++	inactive	vugs, cast	++
VT-6	Heterogeneous	Serial	coarse silt - coarse sand	0.8	8-10%	Qtz (+++), Qtz pol (++), Ms (++), Kfs (+), Pl (+), Gl (r)	sandstones (++), chert (++), acid crystalline rocks (+)	++/+++ (mc)	++	inactive	vugs, cast	+++
VT-7	Heterogeneous	Serial	coarse silt –fine sand	0.3	5-7%	Qtz (+++), Qtz pol (++), Ms (++), Kfs (+), Pl (+), Gl (r)	sandstones (+), chert (+), acid crystalline rocks (r)	+++ (M)	+++	active	vugs, cast	++
VT-8	Moderately homogeneous	Serial	coarse silt - medium sand	0.4	5-8%	Qtz (+++), Qtz pol (++), Ms (++/+), Kfs (+), Pl (+), Gl (r)	acid crystalline rocks (++), sandstones (+), chert (r)	++ (mc)	++	inactive	cast	+++
VT-9	Heterogeneous	Serial	coarse silt –fine sand	0.3	5-8%	Qtz (+++), Qtz pol (++), Ms (++/+), Kfs (+), Pl (+)	acid crystalline rocks (+), chert (+)	+++ (mc)	++	slightly active	vugs, cast	++
VT-10	Heterogeneous	Serial	coarse silt –fine sand	0.3	5-8%	Qtz (+++), Qtz pol (++), Ms (++/+), Kfs (+), Pl (+), Cpx (r)	acid crystalline rocks (r), sandstones (+), chert (r)	+++ (mc)	++	inactive	vugs, cast	+++
VT-11	Heterogeneous	Serial	coarse silt –fine sand	0.25	5%	Qtz (+++), Qtz pol (++), Ms (++), Kfs (+), Pl (+)	acid crystalline rocks (r), chert (r)	+++ (mc)	+++	inactive	vugs, cast	+++
VT-12	Heterogeneous	Serial	coarse silt – medium sand	0.25	5%	Qtz (+++), Qtz pol (++), Ms (++), Kfs (+), Pl (+), Cpx (r)	acid crystalline rocks (r), chert (r)	+++ (mc)	++	inactive	vugs, cast	+++
VD-1	Moderately homogeneous	Bimodal	coarse silt/very fine sand – medium/coarse/very coarse sand (r)	1.5	25-30%	Cpx (+++), Sa (++/+), Pl (+), Grt (+), Am (+), Op (+), Ap (r), Qtz (++/+)*, mica (+)*, K-feldspar (r)*	leucite-bearing tephrites (+++), trachyte and trachy-phonolites (+), quartzarenites (+/r),	+/r (M)	+	inactive	fissures (grains/groundmass)	++ external crust (0.1-0.5 mm)

							acid crystalline rocks (r), chert (r)*					
VD-2	Moderately homogeneous	Bimodal	coarse silt/very fine sand – medium/coarse/very coarse sand (r)	2.5	25-30%	Cpx (+++), Sa (+), Pl (+), Grt (+), Am (+), Op (+), Ap (r), Qtz (++/+)*, mica (+/r)*, K-feldspar (r)*	leucite-bearing tephrites (+/r), trachy-phonolites (r), quartzarenites (+), acid crystalline rocks (r), chert (r)*	+/r (M)	++	inactive	fissures (grains/groundmass)	+++ external crust (0.1-0.3 mm), pore filling
VD-3	Moderately homogeneous	Bimodal	coarse silt/very fine sand – medium/coarse/very coarse sand (r)	1.3	20-25%	Cpx (+++), Lct (++), Sa (r), Pl (r), Grt (r), Am (r), Op (+), Qtz (+)*, mica (+/r)*, K-feldspar (r)*	leucite-bearing tephrites (+), quartzarenites (r), acid crystalline rocks (r), chert (r)*	+/r (M)	++	inactive	fissures (grains/groundmass)	+++ external crust (0.1-0.7 mm), pore filling
VD-4	Moderately homogeneous	Bimodal	coarse silt/very fine sand – medium/coarse/very coarse sand (r)	1.8	20-25%	Cpx (+++), Sa (+), Pl (+), Grt (r), Am (+), Op (+), Kfs (+), Qtz (+), Ol (r), Qtz (+)*, mica (+/r)*, K-feldspar (r)*	leucite-bearing tephrites (+), acid crystalline rocks (r), quartzarenites (r), chert (r)*	r (M)	++	inactive	fissures (grains/groundmass)	+ external crust (0.1-0.5 mm)
VD-5	Moderately homogeneous	Bimodal	coarse silt/very fine sand – medium/coarse/very coarse sand (r)	1.1	20-25%	Cpx (+++), Sa (r), Pl (+/r), Am (++/+), Bt (r), Op (+), Qtz (+)*, mica (+/r)*, K-feldspar (r)*, Grt (+) **	leucite-bearing tephrites (+), trachy-phonolites (r), acid crystalline rocks (r), quartzarenite (+), chert (+/r)*	r (M)	++	inactive	fissures (grains/groundmass)	+ external crust (0.1-0.5 mm)
VD-6	Moderately homogeneous	Bimodal	sporadic finest particles up to very coarse sand	1.9	20-25%	Sa (++/+++), Cpx (++/+++), Bt (+), Am (+), Pl (+), Ol (r), Op (r), Qtz (+)*, mica (+/r)*	trachytic and trachy-phonolites (+/++)	r (M)	++	inactive	fissures (grains/groundmass)	+++ external crust (0.1-1 mm), pore filling
VD-7	Moderately homogeneous	Bimodal	coarse silt/very fine sand – medium/coarse/very coarse sand (r)	2.5	20-25%	Cpx (+++), Sa (+),Am (+/++), Bt (+/r), Pl (r), Grt (r), Op (r), Qtz (+)*, mica (+/r)*, K-feldspar (r)*	leucite-bearing tephrites (+), trachy-phonolites (r), acid crystalline rocks (+), quartzarenites (r)	r (M)	++	inactive	fissures (grains/groundmass)	+ external crust (0.1-0.2 mm), pore filling
VD-8	Moderately homogeneous	Bimodal	coarse silt/very fine sand – medium/coarse/very coarse sand (r)	1.2	15-20%	Cpx (+++), Sa (+), Am (+), Bt (+), Pl (r), Grt (r), Op (r), Qtz (+/++)*, mica (+)*, K-feldspar (r)*	leucite-bearing tephrites (+), trachy-phonolites (r), acid crystalline rocks (+), quartzarenites (r), chert (+/r)*	r (M)	++	inactive	fissures (grains/groundmass)	+++ external crust (0.2-2 mm), pore filling
VD-9	Moderately homogeneous	Bimodal	coarse silt/very fine sand – medium/coarse/very coarse sand (r)	2.2	25-30%	Cpx (+++), Lct (+), Am (r), Bt (r), Op (+), Sa (r), Pl (r), Ap (r), Qtz (+/++)*, mica (r)*, K-feldspar (r)*	leucite-bearing tephrites (++), leucitites (+), trachy-phonolites (r), acid crystalline	R (M)	++	inactive	fissures (grains/groundmass)	++ external crust (0.1-0.4 mm), pore filling

							rocks (+), quartzarenites (r)					
VD-10	Moderately homogeneous	Bimodal	coarse silt/very fine sand – medium/coarse/very coarse sand (r)	2.5	25-30%	Cpx (+++), Sa (r), Am (r), Grt (r), Bt (r), Op (+), Ap (r), Qtz (+)*, mica (r)*, K-feldspar (r)*	leucite-bearing tephrites (+++), leucitites (+), acid crystalline rocks (+/ r)	+/r (M)	++	inactive	fissures (grains/groundmass)	+ external crust (0.1-1 mm)
VC-1 700°	Moderately homogeneous	Serial	coarse silt - coarse sand (sporadic)	1.2	10%	Qtz (+++), Qtz pol (++), Ms (++), Kfs (+), Pl (+), Cpx (r), Ol (?)	acid crystalline rocks (+), chert (+)	++ (L)	-	active	cast, irregular or rounded pores	-
VC-2 700°	Moderately homogeneous	Serial	coarse silt – fine sand	0.5	5-8%	Qtz (+++), Qtz pol (++), Ms (+++/++), Kfs (+), Pl (+), Cpx (r), Gl (r)	acid crystalline rocks (r), chert (r)	++ (M+L rare)	-	slightly active	rounded pores	-
VC-1 800°	Moderately homogeneous	Serial	coarse silt - medium sand	0.4	10%	Qtz (+++), Qtz pol (++), Ms (++), Kfs (+), Pl (+)	acid crystalline rocks (+), chert (+)	++ (mc)	-	inactive	cast	-
VC-2 800°	Moderately homogeneous	Serial	coarse silt - medium sand	0.4	10-15%	Qtz (+++), Qtz pol (++), Ms (+++/++), Kfs (+), Pl (+), Cpx (r)	acid crystalline rocks (+), chert (+)	++ (mc)	-	inactive	cast	-
VC-1 900°	Moderately homogeneous	Serial	coarse silt - medium sand	0.4	10-15%	Qtz (+++), Qtz pol (++), Ms (++), Kfs (+), Pl (+)	acid crystalline rocks (+), chert (+)	++ (mc)	-	inactive	cast	-
VC-2 900°	Moderately homogeneous	Serial	coarse silt - coarse sand	0.6	10-15%	Qtz (+++), Qtz pol (++), Ms (+++/++), Kfs (+), Pl (+), Cpx (r)	acid crystalline rocks (+), chert (+)	++ (mc)	-	inactive	cast	-

Legend: (+++) prevalent, (++) common, (+) sporadic, (r) rare; MGS = Maximum Grain Size; Cpx = Clinopyroxene; Kfs = K-Feldspar; Sa= Sanidine; Lct = Leucite; Grt = Garnet; Am = Amphibole; Pl = Plagioclase; Ms = Muscovite; Qtz = Quartz monocrystalline; Qtz pol = Quartz polycrystalline; Ol = Olivine; Bt = Biotite; Op = opaque minerals; Ap = apatite. (*) = mineralogical phases and / or lithic fragments present exclusively as aplastic inclusions of small size (very fine sand and coarse silt) and homogeneously diffused in the original clayey matrix. (**) = large crystals of black melanite garnet.

Table S2 – Supplementary Material. Average major element concentrations (Avg) (wt%), standard deviations (St Dev) and calculated structural formulae (in a.p.f.u. on the basis of 6 oxygens) of clinopyroxene inclusions of five *dolia* samples.

	VD4 (n=6)	St Dev	VD5 (n=3)	St Dev	VD6 (n=3)	St Dev	VD7 (n=7)	St Dev	VD8 (n=3)	St Dev
SiO_2	48.90	2.75	48.19	1.34	48.51	1.38	47.34	1.90	46.41	1.86
TiO_2	1.39	0.52	1.46	0.14	0.80	0.41	1.55	0.23	1.65	0.35
Al_2O_3	6.91	2.14	7.27	1.54	5.73	0.89	7.90	1.11	6.83	0.94
FeO	6.99	2.33	7.26	1.20	8.41	1.94	8.85	2.43	8.65	1.56
MnO	0.00	0.00	0.00	0.00	0.00	0.00	0.00	0.00	0.00	0.00
MgO	13.59	2.45	12.73	1.39	12.98	1.66	11.64	1.76	11.39	0.92
CaO	21.45	0.32	21.51	0.27	21.50	0.58	21.41	0.78	23.73	0.15
Na_2O	0.77	0.35	1.59	0.32	2.06	1.15	1.31	0.46	1.35	0.15
Cr_2O_3	0.00	0.00	0.00	0.00	0.00	0.00	0.00	0.00	0.00	0.00
Total	100.00		100.00		100.00		100.00		100.00	
Si	1.80	0.08	1.77	0.04	1.78	0.05	1.75	0.06	1.72	0.06
Ti	0.04	0.01	0.04	0.00	0.02	0.01	0.04	0.01	0.05	0.01
Al	0.30	0.10	0.31	0.07	0.25	0.04	0.34	0.05	0.30	0.04
Fe^{2+}	0.14	0.08	0.04	0.08	-0.05	0.13	0.12	0.08	0.00	0.02
Fe^{3+}	0.08	0.10	0.18	0.06	0.30	0.19	0.16	0.08	0.27	0.05
Mn	0.00	0.00	0.00	0.00	0.00	0.00	0.00	0.00	0.00	0.00
Mg	0.74	0.13	0.70	0.07	0.71	0.09	0.64	0.09	0.63	0.05
Ca	0.85	0.02	0.85	0.01	0.84	0.02	0.85	0.03	0.94	0.01
Na	0.06	0.03	0.11	0.02	0.15	0.08	0.09	0.03	0.10	0.01
Cr	0.00	0.00	0.00	0.00	0.00	0.00	0.00	0.00	0.00	0.00
Total	4.00		4.00		4.00		4.00		4.00	
Wo	46.87	1.71	47.93	1.18	46.62	1.03	48.09	1.00	51.22	0.72
En	41.11	5.97	39.41	3.46	39.10	4.26	36.33	4.90	34.21	2.74
Fs	12.03	4.31	12.66	2.35	14.29	3.61	15.58	4.56	14.56	2.58
Mg#	0.7714	0.0879	0.7562	0.0501	0.7319	0.0702	0.6994	0.0895	0.7013	0.0530
Fe_2O_3	3.06		5.68		3.76		4.96		8.64	
FeO	4.40		2.80		3.22		4.68		0.61	

Legend: Wo = wollastonite, En = enstatite, Fs = ferrosilite, Mg# = [Mg/(Mg+ Fe_T+Mn)].

Table S3 – Supplementary Material. Trace element concentrations of representative clinopyroxenes (cpx) from the studied *dolia*.

Sample code	VD4_1	VD4_2	VD4_3	VD4_4	VD4_5	VD5_1	VD5_2	VD5_3	VD6_1	VD6_2	VD6_3	VD7_1	VD7_2	VD7_3	VD7_4	VD7_5	VD7_6	VD8_1	VD8_2	VD8_3
Sc		82	32	107	70	77	54	55	54	86	28	49	63	71	20	99	16	54	91	82
V	211	101	191	104	154	109	186	171	305	247	301	199	133	158	328	116	280	245	126	164
Cr	272	56	19	559	37	125	144	86	15	452	19	6	41	13		38	56	25	19	84
Co	36	24	33	24	32	28	30	33	41	41	21	36	28	31	37	26	35	41	31	35
Sr	375	168	459	161	195	318	309	321	316	189	405	247	149	190	575	204	578	528	270	406
Y	39	20	40	19	31	24	37	35	38	22	61	33	19	27	67	20	47	52	23	41
Zr	324	116	399	106	222	210	334	297	199	93	429	285	95	177	677	241	479	583	170	340
Nb	3	0	4	0	1	1	2	2	1	0	1	1	0	1	9	1	5	4	1	4
Ba		6	4	4	5	14	8	6	5	20	6	4	1	1	5	1	0	1	4	4
La	43	15	50	25	22	25	31	36	25	13	51	26	11	20	86	17	58	64	19	42
Ce	134	52	150	56	79	83	111	116	93	45	186	91	41	71	255	62	179	194	66	134
Pr	18	8	22	10	13	13	18	18	15	8	30	15	7	12	36	10	25	29	11	21
Nd	86	43	93	45	65	64	86	84	79	45	153	82	40	63	158	53	112	139	56	104
Sm	10	11	21	10	20	14	21	18	20	12	34	20	9	15	31	15	22	27	13	24
Eu	4	3	5	2	4	3	5	5	3	3	6	4	2	4	8	3	5	7	3	6
Gd	19	10	17	8	14	10	15	16	14	7	22	14	8	11	26	12	14	23	10	18
Tb		1	2	1	2	1	2	2	2	1	3	2	1	1	3	1	2	3	1	2
Dy	15	5	10	5	9	6	10	9	9	6	16	8	5	8	18	5	12	14	7	10
Ho	1	1	1	1	1	1	2	1	2	1	3	1	1	1	2	1	2	2	1	2
Er	1	2	4	2	3	2	3	3	3	1	7	3	2	2	7	2	5	5	2	4
Tm		0	0	0	0	0	0	0	0	0	1	0	0	0	1	0	1	1	0	0
Yb		1	3	2	1	1	2	2	3	2	5	2	1	2	5	2	4	4	2	3
Lu		0	0	0	0	0	0	0	0	0	1	0	0	0	1		0	0	0	0
Ta	1	0	1	0	0	0	1	1	0	0	0	0	0	0	2	0	1	1	0	1
Pb		1	2	1	0	0	2	4	10	3	2	1	1	1	2		1	1	1	3
Th		1	2	1	1	1	1	1	1	0	2	1	0	1	3	1	1	3	1	2
U		0	0	0	0		2	0			0	0	0	0	0	0	0	0	0	0
Sb	5	0		1	0			1	1		1				2	4	0	0		
Rb		1	5	2	1	1	3	3		2	1	0	0		3	2		0		1
Cs		0	0	0	0	1	0	0		0	0		0	0	0		0	0		0
Ni		46	20	69	48	52	21	42		80		13	59	47	13	42	14	34	49	48
La/Sm	4	1	2	2	1	2	1	2	1	1	1	1	1	1	3	1	3	2	1	2
La/Yb		19	15	10	15	31	19	21	9	6	10	13	9	11	17	7	16	15	12	13
Sm/Yb		14	6	4	14	18	13	11	7	5	7	10	7	9	6	6	6	6	8	7
Ce/Nd	2	1	2	1	1	1	1	1	1	1	1	1	1	1	2	1	2	1	1	1
Ce/Tm		166	354	647	217	628	249	250	191	599	264	236	198	247	322	127	356	340	274	332
Nd/Tm		137	220	518	180	480	191	182	160	600	217	214	192	220	199	108	223	244	234	258
Ce/Lu		263	371	320	349	321	497	580	212	240	264	350	275	304	344		412	432	439	477
Nd/Lu		216	231	256	289	246	382	421	179	241	217	316	266	270	213		258	309	375	370
Zr/Y	8	6	10	6	7	9	9	9	5	4	7	9	5	7	10	12	10	11	8	8
Ce/Y	3	3	4	3	3	4	3	3	2	2	3	3	2	3	4	3	4	4	3	3

CRediT author statement:

G. Montana: Formal analysis, Investigation, Writing - Original Draft, Writing - Review & Editing, Supervision; **L. Randazzo:** Formal analysis, Investigation, Writing - Original Draft, Writing - Review & Editing; **B. Barca:** Formal analysis, Investigation; **M. Carroll**: Writing - Original Draft, Writing - Review & Editing, Conceptualization, Supervision, Funding acquisition.